Numerical Study of the Urban Heat Island in Sendai City with Potential Natural Vegetation and the 1850s and 2000s Land-Use Data

Lidia Lazarova VITANOVA

Graduate School of Life and Environmental Sciences, The University of Tsukuba, Tsukuba, Japan

Hiroyuki KUSAKA

Center for Computational Sciences, The University of Tsukuba, Tsukuba, Japan

Van Quang DOAN

Center for Computational Sciences, The University of Tsukuba, Tsukuba, Japan

and

Akifumi NISHI

Graduate School of Life and Environmental Sciences, The University of Tsukuba, Tsukuba, Japan

(Manuscript received 24 December 2017, in final form 2 November 2018)

Abstract

In this study, we investigated the impact of urbanization on surface air temperatures and the urban heat island (UHI) for Sendai City. We estimated the impact of urbanization during the 150-year period by comparing the 1850s to the 2000s case. We used the Weather Research and Forecasting (WRF) model with 1-km horizontal resolution and three land-use datasets: one for potential natural vegetation (PNV) data, and the other two for realistic land-use data (the 1850s and 2000s). First, the results from the control simulation (2000s land-use case) were verified against observations. The results show that the WRF model reasonably reproduced the diurnal variation of the observed surface air temperatures in the 2000s land-use case at six stations of the Miyagi prefecture. The model mean biases ranged from −0.29 to −1.18°C in August (10-year average) and from −0.44 to −1.50°C in February (10-year average). Second, the impact of urbanization on the surface air temperature distribution in and around Sendai City was evaluated. For the 1850s land-use case, the very small urban area of Sendai City led to a negligible UHI. Note that this case yields nearly the same surface air temperatures as experiments using PNV. If we compare the simulated monthly mean surface air temperatures in the central part of Sendai City between the 1850s and 2000s land-use cases, we find that the monthly mean temperature for February in the 2000s is 1.40°C higher than that in the 1850s, whereas that for August is 1.30°C. Similarly, we find a considerable nocturnal (1800−0500 JST) average surface air temperature increase of 2.20°C in February and 2.00°C in August.

Keywords urban heat island; urbanization; potential natural vegetation; land-use change; Weather Research and Forecasting model

Corresponding author: Hiroyuki Kusaka, Center for Computational Sciences, University of Tsukuba, 1-1-1, Tennodai, Tsukuba, Japan
E-mail: kusaka@ccs.tsukuba.ac.jp
J-stage Advance Published Date: 16 November 2018

Citation Vitanova, L. L., H. Kusaka, V. Q. Doan, and A. Nishi, 2019: Numerical study of the urban heat island in Sendai City with potential natural vegetation and the 1850s and 2000s land-use data. *J. Meteor. Soc. Japan*, **97**, 227–252, doi:10.2151/jmsj.2019-013.

1. Introduction

Urbanization has attracted considerable interest in recent years and plays an important role in people's lives. In the past few decades, many cities have witnessed a rapid rise in atmospheric temperature because of rapid urbanization and industrialization. Thus, considerable attention has been paid to urban heat islands (UHIs) as representative of climate modification in urban areas. UHIs are generally defined as the difference in surface air temperature between a city and its surrounding rural area. This difference strongly depends on geographical location, population, anthropogenic heat (AH) release, city size, weather, and seasonal variations (Oke 1973, 1982). The increase in temperature of urban areas has led to human discomfort, health problems, higher energy consumption, and pollution (Gartland 2012).

Recently, many numerical experiments have been used to explore the impact of past urbanization on UHIs for various cities (e.g., Kusaka et al. 2000, 2014; Ichinose 2003; Lin et al. 2008; Miao et al. 2009; Shem and Shepherd 2009; Zhang et al. 2009; Kitao et al. 2009; Georgescu et al. 2009a, b, 2011; Grossman-Clarke et al. 2010; Zhang et al. 2010; Zhou and Shepherd 2010; Aoyagi et al. 2012; Cui and De Foy 2012; Feng et al. 2012; Salamanca et al. 2012; Yang et al. 2012; Giannaros et al. 2013; Li et al. 2013; Doan and Kusaka 2015; Heaviside et al. 2015; Sugimoto et al. 2015a; Bhati and Mohan 2016; Chen et al. 2016; Li et al. 2017; Vitanova and Kusaka 2018). For the northern areas of the Tokyo metropolitan area, Kusaka et al. (2000) estimated the effect of land-use alteration over 85 years (1900–1985) on the sea breeze and UHI using historical land-use data from the 1900s, 1950s, and 1985. They concluded that the intensity of daytime UHI in this area on a clear sky summer day was 3.0–4.0°C because of heat advection, land-use changes, and delays in the sea-breeze front over the urban area. For Atlanta, between 1984 and 2007, Zhou and Shepherd (2010) numerically examined the UHI and summertime heat waves. They identified that the largest UHI magnitude occurred in spring. For Phoenix, between 1973 and 2005, Grossman-Clarke et al. (2010) confirmed the UHI effect at night. They identified that the effect increased when the irrigated agricultural land was converted to a suburban development area. For Ho Chi Minh City, between 1989 and 2009, Doan and Kusaka (2015) identified the simulated urbanization impact to be 0.31°C in April, with an overall 0.64°C increase in surface air temperature during this period. They argued that urbanization contributed approximately half of the temperature increase. For Hokkaido, Sugimoto et al. (2015a) investigated the impact of historical land-use change on the surface air temperature. They used long-term observations and a regional climate model based on past and current land-cover maps. They identified a greater rate of warming in winter than in summer and a greater increase in daily minimum than daily maximum temperatures. Moreover, their results suggested that urbanization had a strong influence on the historical temperature increase.

Note that the impact of future urbanization on UHI has been extensively studied (e.g., Shepherd et al. 2010; Salathé et al. 2010; Adachi et al. 2012; Argüeso et al. 2012, 2014; Kusaka et al. 2012, 2016; Hamdi et al. 2014; Iizuka et al. 2015; Doan et al. 2016; Chen and Frauenfeld 2016; Lee et al. 2017; Kaplan et al. 2017). For example, Argueso et al. (2014) used data from 1990 to 2009 and future data from 2040 to 2059 to examine the impact of future urban expansion in Sydney. For Brussels and the greater Paris region, Hamdi et al. (2014) studied the present climate from 2001 to 2010 and the future climate from 2046 to 2055. Most studies identified a large temperature increase with future urbanization. However, Kusaka et al. (2016) investigated urban climate projections for Tokyo for August in the 2050s. For such a mature metropolis, they identified that increase in temperature because of urbanization would be much lesser than that from global climate change.

Although previous studies have investigated the impact of urbanization on the local climate of a city, few studies have tracked this impact from the establishment of the city itself. Moreover, very few of them are numerical studies that focus on the climate effect between the potential natural vegetation (PNV) data and realistic land-use changes. PNV is "untouched" vegetation that would exist in the absence of humans, whereas realistic land-use is represented by the 1850s and 2000s land-use cases, which include the human

influence over cities and vegetation. Kitao et al. (2009) investigated the impact of urbanization for the Osaka metropolitan area using PNV and current land-use data (2006). They concluded that the inland air temperature on a clear sky day under the current land use was ~ 4°C higher than that under the PNV land-use near the Osaka Plain and Southern Kyoto. Ichinose (2003) numerically investigated urban warming related to land-use changes for 135 years (1850–1985) for five Japanese cities, including Sendai City. However, each of these studies separately focused on the impact of land-use change between PNV and present and between 1850 and 1985, and the simulations were limited to several typical summer days.

Here, we examine the impact of urbanization on the UHI in Sendai City during the 1850s. We then compare it with simulated results using PNV. Additionally, we estimate the impacts of the urbanization during this 150-year period by comparing the 1850s to the 2000s case. Moreover, we investigate the individual contributions between AH release and land-use changes. There are two primary reasons for studying Sendai City. First, Sendai City, known as the "city of trees", is one of the greenest Japanese cities. It has numerous tree-lined streets and green areas. Most other studies have focused on cities with lesser vegetation; however, studies focusing on cities with plenty of vegetation should not be ignored. Second, estimating the impact of past urbanization could contribute to improved urban planning for Sendai City, particularly because it was damaged by the Great East Japan Earthquake of 2011. The plan should include mitigation strategies for the thermal environment as the temperature is expected to increase in the next several decades because of global warming. Moreover, the possibility of a large earthquake and subsequent disasters in the future requires wider examination of Sendai and its surrounding areas, including the past, present, and future urbanization impact on UHIs. For example, Iizuka et al. (2015) showed a better urban future planning solution for the Nagoya metropolitan area by considering UHI mitigation and tsunami protection using regional climate simulations.

Thus, our study focuses on the natural and anthropogenic influences on the local climate in Sendai City, which may be useful for the field of physical geography.

In the next section, we describe the data and methodology. Results are given in Section 3. Discussion is followed in Section 4, and we summarize the conclusion in Section 5.

2. Data and methodology

2.1 Study area

In 1889, Sendai was incorporated as a city with a population of 86,000, an expanse of 17.5 km^2, and a population density of 4,928 people km^{-2} (Urban Planning Bureau, Sendai City 2015). Since then, the city has grown quickly; it has subsequently merged with many surrounding towns, increasing its population to 1,009,078 in 2000. The city area expanded to 788.0 km^2 and the population density increased to 1,280 people km^{-2} in 2000 (City of Yokohama 2000: Population News of Major Cities).

Note that Sendai City has a diverse geography and is surrounded by mountains and the ocean (Fig. 1). The city's borders are defined by the Ou Mountain range in the west and the Pacific Ocean to the east. The elevation gradually changes from a plain in the east to a hilly center as you move toward the mountains in the west. The city's location is 38.16°N, 140.9°E with an average elevation of 44 m.

As per the Köppen–Geiger system, Sendai City is has a humid subtropical climate zone (Kottek et al. 2006; Peel et al. 2007), i.e., it experiences a hot summer and cold winter. August is the warmest month, with a mean surface air temperature of 24.20 °C, whereas January and February are the coldest months with mean temperatures of 1.60 and 2.00°C, respectively (Japan Meteorological Agency 2016).

2.2 Model configurations

To evaluate the impact of past and present urbanization, numerical simulations were run for August and February using the Weather Research and Forecasting (WRF) model 3.5.1 (Skamarock et al. 2008) with 1-km resolution. Such a high resolution is beneficial to detect grid cells of a very small urban area and provides a wealth of high-resolution output data.

Most classical UHI studies have focused on the nocturnal heat island observed on clear calm days during summer and winter (Kusaka 2008). Moreover, the increased energy consumption for cooling or heating could be an important factor for the temperature behavior during summer and winter. Hence, to investigate this behavior, we selected the warmest (August) and coldest (February) months for our study.

The overall model configurations are summarized in Table 1. For the numerical experiments, four nested domains with spatial resolutions of 27, 9, 3, and 1 km are used. Thirty vertical layers are used for all domains. Figure 1a shows the simulation domains in which domain d04 corresponds to the researched area

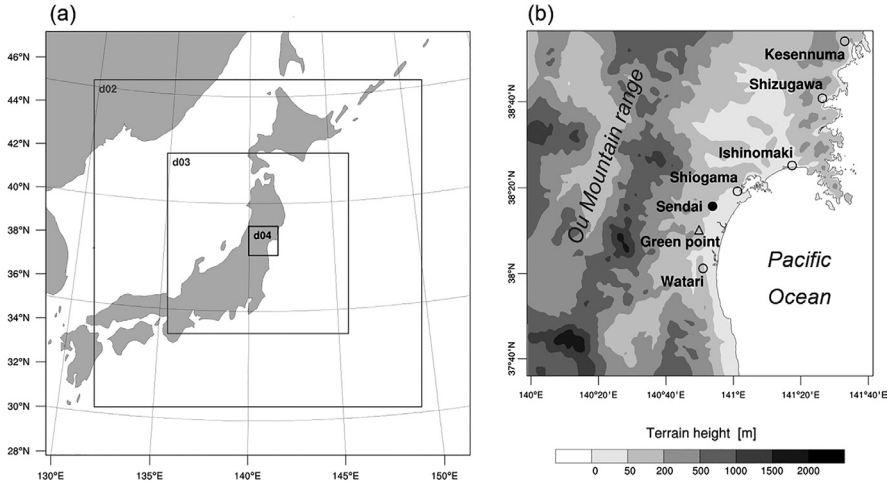

Fig. 1. Study area. (a) The first (d01), second (d02), third (d03), and fourth (d04) domains used in the WRF model. (b) The terrain height (m) in the fourth domain (d04) and locations of the AMeDAS weather stations. The closed black circle represents the Sendai observatory, the triangle represents a rural site, and the open circle represents surrounding observatories in the other urban areas.

Table 1. Model configurations.

	Domain 01	Domain 02	Domain 03	Domain 04
Model version	WRF3.5.1-ARW			
Runtime in August	25 July 2100 to 01 September 0300 (JST) 2000–2009			
Research period in August	1 August 0100 to 31 August 2400 (JST) 2000–2009			
Runtime in February	20 January 2100 to 01 March 0300 (JST) 2000–2009			
Research period in February	1 February 0100 to 28 February 2400 (JST) 2000–2009			
Parent data	NCEP Final Analysis dataset every 6 hours			
Grid spacing (km)	27	9	3	1
Grid cell numbers	80 × 80	184 × 184	304 × 304	147 × 147
The number of vertical layers	30 layers			
Land surface model	Noah-LSM (Chen et al. 2011)			
Urban canopy model	Single-layer/UCM (Kusaka et al. 2001; Kusaka and Kimura 2004)			
Microphysics	WSM 6-class graupel scheme (Hong et al. 2004)			
Turbulence	Mellor-Yamada-Janjic TKE scheme (Janjić 1994)			
Shortwave radiation	Dudhia Shortwave scheme (Dudhia 1989)			
Longwave radiation	RRTM scheme (Mlawer et al. 1997)			
Cumulus	Kain–Fritsch scheme (for d01 only) (Kain 2004)			

in this study (Fig. 1b).

The initial and boundary conditions are based on the final operational and global analysis data obtained from the National Center for Environmental Prediction (NCEP-FNL). These data include the sea surface temperature and are converted from the Universal Time Coordinated (UTC) to the Japanese Standard Time (JST; UTC+9 hours). The simulation period lasted from 25 July (2100 JST) to 01 September (0300 JST) and from 20 January (2100 JST) to 01 March (0300 JST) between 2000 and 2009 (10 years). The research period used for analysis lasted from 1 August (0100 JST) to 31 August (2400 JST) and from 1 February (0100 JST) to 28 February (2400 JST) between 2000 and 2009.

To justify the physical lower boundary for the WRF model, we use the Noah land-surface model (Chen and Dudhia 2001) coupled with the single-layer urban

canopy model (UCM) (Kusaka et al. 2001; Kusaka and Kimura 2004; Chen et al. 2011). The single-layer UCM calculates the urban surface fluxes and temperature, considering a two-dimensional urban canyon for roofs, buildings, and roads. All experimental cases use the same physics scheme.

2.3 Experimental cases and land-use data

To estimate the impact of urbanization on surface air temperature and UHI in Sendai City, we considered the following experimental cases. Table 2 lists their parameters.

a. Case PNV

PNV is vegetation without any human intervention. Miyawaki et al. (1987) investigated numerous sites throughout Japan that are affected by human activities. In this study, we digitized the PNV map which was created by Miyawaki and Okuda (1975) and Geographical Survey Institute (1977), and then we interpolated it in the WRF model. To estimate the impact of urbanization on the surface air temperature, we compare the PNV to the 1850s and the 1850s to the 2000s. Comparing the natural experiment to the urban one is commonly used for modeling studies (Ma et al. 2017). For example, Georgescu et al. (2011) used this approach while replacing all anthropogenic land cover with native vegetation.

b. Case LU1850s

Case LU1850s is a realistic land-use during the 1850s. We utilized the 1850s map, which was created by Arizono (1995) and Himiyama (1995). We converted the map-image for the 1850 map to digital data. Then, as in the previous case, the data are interpolated in the model with AH set to 0 W m^{-2}.

c. Case 1850s

For this case, the converted digital data are the same as in the LU1850s case. However, a comparison between the LU1850s and 1850s cases is required to clarify the uncertainty of AH impact in the 1850s. We assumed that the AH values in the 1850s probably range between 0 and 5 W m^{-2}. We also assumed that the accumulated heat is less for this period because there was no electricity or cars. However, the AH may be nonzero because Japan opened up for commerce and influence with other countries in this period, although industrialization had just begun. Hence, we assumed that the AH in the 1850s was comparable to that in the rural area in Japan at present (5 W m^{-2}).

In this case, wooden houses and buildings with ~ 5-m height are considered.

d. Case LU2000s

This realistic case uses land-use data from 2006. The land-use data are provided by the Japanese National Land Numerical service. The AH data used for this case were set to 0 W m^{-2}. We will use the results from this case to evaluate the impact of land-use changes and anthropogenic heat release because of the recent human activities in Sendai City.

e. Case 2000s

In this case, the land-use data are the same as in the LU2000s case. However, the AH data used for the 2000s case is explained in detail in Section 2.4.

The d04 area is divided into 147 × 147 horizontal grid points. The LU1850s and 1850s cases have only one urban category, and the average urban fraction is estimated using an old detailed Sendai City map, which was created by Aizawa (1892). To quantify the urban fraction for the 2000s case, we defined three primary categories: low residential (LR), medium residential (MR), and high residential/commercial (HR) area.

Figure 2 shows diagrams of the land-use data associated with the PNV, LU1850s, 1850s, LU2000s, and 2000s cases. The central city site (CCS) indicates the closest grid point to an observation station at Sendai City. The CCS in every land-use case falls under a different land-use category. The CCS is a forest for the PNV (Fig. 2a), but is urban for LU1850 and 1850s (Fig. 2b) and for LU2000s and 2000s (Fig. 2c). Traditionally, UHIs are detected by comparing two fixed points in the urban and rural areas. However, the urban area is strongly affected by the influence of the surrounding areas. Hence, only one point is insufficient to identify the UHI for the whole city, particularly large cities composed of different land-use categories. To overcome this problem, we have considered estimating the UHI for both CCS and the total city area (TCA). In this study, the TCA represents the current total city area of the Sendai metropolis. While the TCA of the PNV is a forest, that of the LU1850s and 1850s cases comprises urban and non-urban areas (mostly irrigated cropland), and that of the LU2000s and 2000s cases comprises LR, MR, and HR areas. The number of grids used for CCS and TCA is shown in Table 2. Moreover, Table 2 shows the urban fraction and urban parameters for the LU1850s, 1850s, LU2000s, and 2000s cases. We used these parameters as input variables for the UCM.

There are small differences in areas located along

Table 2. Summary of simulation cases.

	Name of simulation case	PNV	LU1850s	1850s	LU2000s			2000s		
	Land-use (LU) category	Vegetation	Urban	Urban	Low Residential (LR)	Medium Residential (MR)	High Residential (HR)	Low Residential (LR)	Medium Residential (MR)	High Residential (HR)
Land-use	Land-use data	PNV	1850				2006			
Anthropogenic Heat (AH)	AH in August (W m^{-2})	–	0.00	5.00	0.00	0.00	0.00	21.72	36.03	49.27
	AH in February (W m^{-2})	–	0.00	5.00	0.00	0.00	0.00	30.85	51.17	69.98
Number of Grids in Sendai City	Number of urban grids for each LU category	–	14		350	254	91	350	254	91
	Number of grids used for CCS					1				
	Number of grids used for TCA					695				
Urban Fraction	Range of urban fraction (%)	–	0.01–1.00		0.05–0.55	0.55–0.85	0.85–1.00	0.05–0.55	0.55–0.85	0.85–1.00
	Average urban fraction for each LU category (%)	–	0.67		0.41	0.68	0.93	0.41	0.68	0.93
	Building coverage ratio of one grid (%)	–	0.29		0.15	0.25	0.34	0.15	0.25	0.34
Other Urban Parameters	Building height (m)	–	5.00		6.80	8.60	19.80	6.80	8.60	19.80
	Roof width (m)	–	7.00		11.56	14.62	33.66	11.56	14.62	33.66
	Road width (m)	–	9.00		19.65	24.85	57.22	19.65	24.85	57.22
	Heat capacity of roof (J m^{-3} K^{-1})	–	1.65×10^6		1.14×10^6	1.94×10^6	2.11×10^6	1.14×10^6	1.94×10^6	2.11×10^6
	Heat capacity of building wall (J m^{-3} K^{-1})	–	1.52×10^6		1.46×10^6	1.66×10^6	1.89×10^6	1.46×10^6	1.66×10^6	1.89×10^6
	Heat capacity of ground (J m^{-3} K^{-1})	–	1.09×10^6		1.94×10^6	1.94×10^6	1.94×10^6	1.94×10^6	1.94×10^6	1.94×10^6
	Thermal conductivity of roof (J m^{-1} s^{-1} K^{-1})	–	0.50		0.50	1.18	1.51	0.50	1.18	1.51
	Thermal conductivity of building wall (J m^{-1} s^{-1} K^{-1})	–	0.19		0.43	0.87	1.13	0.43	0.87	1.13
	Thermal conductivity of ground (J m^{-1} s^{-1} K^{-1})	–	0.20		0.75	0.75	0.75	0.75	0.75	0.75
	Surface albedo of roof (fraction)	–	0.20		0.20	0.20	0.20	0.20	0.20	0.20
	Surface albedo of building wall (fraction)	–	0.20		0.20	0.20	0.20	0.20	0.20	0.20
	Surface albedo of ground (fraction)	–	0.20		0.20	0.20	0.20	0.20	0.20	0.20

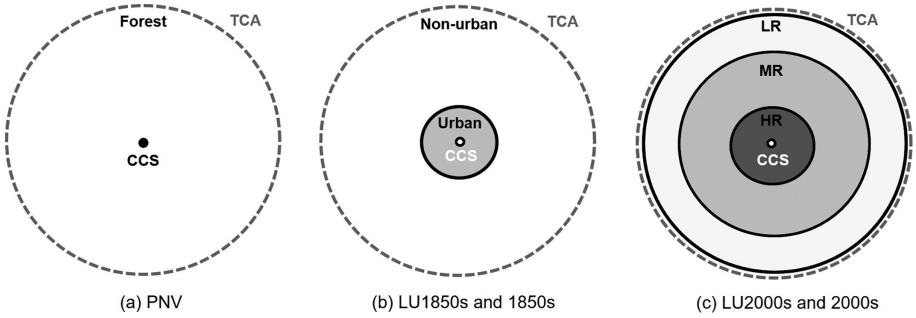

Fig. 2. Land-use types in Sendai City for the various cases. (a) PNV. (b) LU1850s and 1850s. (c) LU2000s and 2000s. LR, MR, and HR are low, medium, and high residential area. CCS is central city site, and TCA is total city area.

inland lakes and rivers because of the different expansion of the water surface data between the PNV and 1850s original maps. However, these differences do not affect the results of the study.

2.4 *Anthropogenic heat flux data*

The AH is an important input for urban climate simulations. In the 2000s case, the total AH flux released QF (W m^{-2}) was estimated from heat from vehicles, QV; heat from buildings, QB; and human metabolic, QM heat. Note that QB is equal to the heat released from electricity, QBE, and from heating fuels, QBH. The QBE value is calculated from the total electricity consumption data obtained by the Tohoku Electric Power. Note that QBH is calculated from the total gas, kerosene, LPG, naphtha, gas oil, and coal consumption data obtained by Sendai City Gas and the Ministry of Economy, Trade and Industry of Japan. The average released QM is assumed to be 100.00 W per person (Sailor and Lu 2004; Sailor et al. 2015). Moreover, QV is calculated from gasoline data provided by the Ministry of Economy, Trade and Industry. The present study uses a simple equation to define the QF (Sailor and Lu 2004):

$$QF = QV + QB + QM,$$
$$QB = QBE + QBH.$$

To calculate the total AH, we multiplied the monthly (August and February) average electricity, gas, kerosene, LPG, naphtha, gas oil, coal, and gasoline consumption data by the population of Sendai City. Then, we divided it by the area of the city (total number of model grid cells in Sendai City). Consequently, we obtained the degree of AH released for each model grid cell, and then we converted it to the heat flux amount.

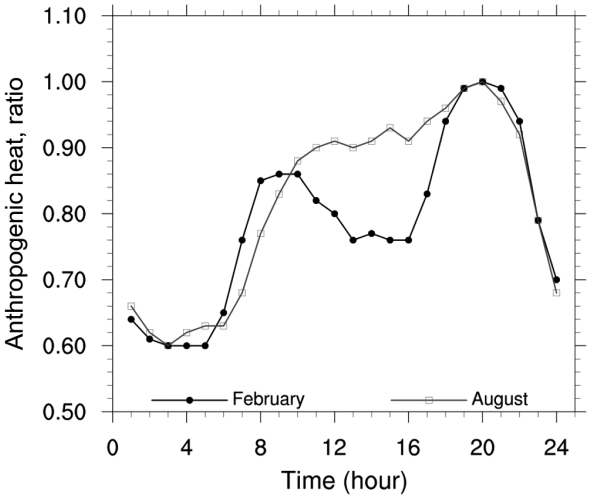

Fig. 3. Diurnal variation of total anthropogenic sensible heat flux (AH). The horizontal axis indicates the time (hour) and the vertical axis indicates the ratio of AH at each hour to the maximum AH. The black line with closed circles and gray line with open squares indicate the AH in February and August, respectively. The max AHs are 50.4 and 35.5 W m^{-2} in February and August, respectively.

In addition, we estimated the diurnal profile of the AH in August and February. For the estimate, we separately calculated the diurnal profiles of the QV, QB, and QM, and then the diurnal profile of AH was calculated as a weighted average of these three diurnal profiles. The weights of QV, QB, and QM are 0.64, 0.24, and 0.12 for August and 0.58, 0.32, and 0.10 for February, respectively. Figure 3 shows that the maximum values in August and February occur at 2000

JST. The diurnal variation of QV and QB was determined using hourly data. For QM, the diurnal variation of metabolic heat emission was assumed to be 100.00 W averaged per person: 75.00 W per person at night (2300–0500 h) and 175.00 W per person in daytime (0700–2100 h) (Sailor and Lu 2004).

2.5 Observational meteorological data

For the present study, the observational data that was used is the automated meteorological data acquisition system (AMeDAS) network data provided by the Japan Meteorological Agency. Moreover, it was measured in Sendai City and in at stations near the city in Miyagi prefecture. The meteorological data was sampled hourly and included the surface air temperature, wind speed, and wind direction for August and February from 2000 to 2009.

3. Results

3.1 Land-use change in Sendai City

The PNV case is characterized by three main types of vegetation: evergreen broadleaf forest, deciduous broadleaf forest, and evergreen needleleaf forest (Fig. 4a). The evergreen broadleaf forest covers the coastal area up to 700 m above sea level, whereas the deciduous broadleaf forest covers the area between 700 and 1500 m above sea level and decreases with elevation (Miyawaki 1984). The mountain area is characterized by an evergreen needleleaf forest at an elevation of 1600 m above sea level and covers a very small region because of the limited extent of mountains in the Sendai area.

The land-use of the 1850s is shown in Fig. 4b, in which the region in red indicates the urban area.

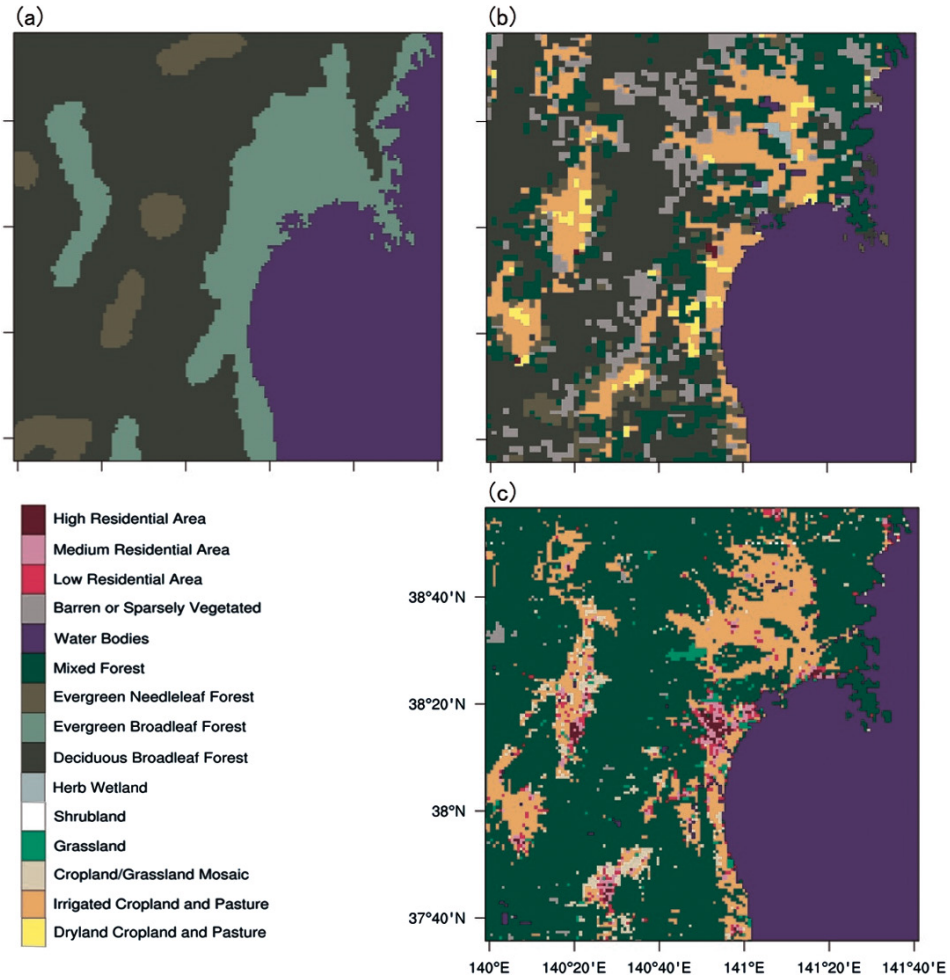

Fig. 4. Land-use around Sendai city for (a) PNV, (b) 1850s, and (c) 2000s cases.

Here the evergreen broadleaf forest has drastically decreased, and the irrigated cropland has increased because of human intervention. Moreover, numerous mixed forest and barren areas appear near the cropland, and the deciduous broadleaf forest area is reduced.

In the 2000s case, the urban area of Sendai City shows a considerable increase over that in the 1850s and is surrounded by irrigated cropland. Also, the evergreen broadleaf forest area is very limited (Fig. 4c).

3.2 Model evaluation

We evaluate the model by comparing the observed (OBS) and simulated (WRF) data. The simulated results were obtained by extracting data from the grid point closest to the observation weather station. The surface air temperature and wind measurements used for the validation are discussed below.

a. Surface air temperature

To check the accuracy of the diurnal variation of the simulated surface air temperature, we used meteorological observation data from six stations. As described in Table 3 and Fig. 1b, the location of each station belonged to an urban category. The locations for Sendai City and Ishinomaki corresponded to the HR area. Shiogama and Kesennuma belonged to the MR area, whereas Shizugawa and Watari were located in the LR area. Moreover, in Fig. 1b, we used the location named "green point". As all these locations belonged to the urban area, this green point was located in an evergreen broadleaf forest area, and the land-use category of this area remained the same for all the PNV, LU1850, 1850s, LU2000s and 2000s cases. We will use this point to compare the surface air temperature between all land-use cases in the non-urban area.

The WRF results show sufficient correlation with the OBS data with correlation coefficients exceeding 0.97 for all the observed data (Table 3). The biases ranged from −0.29 to −1.18°C in August and from −0.44 to −1.50°C in February; however, in February, there is a tendency to have a strong cold bias except at Ishinomaki. Moreover, we considered the possibility of AH being underestimated in the LR area (Figs. 5f, 6e, f) because the range of urban fraction (0.05–0.55) used in the LR area should be larger, which will increase the average urban fraction (Table 2).

In Sendai City, the lowest surface air temperatures (21.80 and 0.05°C) are observed at 0500 and 0600 JST in August and February, respectively, while the highest temperatures (26.19 and 5.11°C) are observed at 1300 and 1400 JST in August and February, respectively (Figs. 5, 6). Moreover, Fig. 5 shows that the observed surface air temperatures in August at 0500 JST are less in Ishinomaki, Shiogama, Kesennuma, Shizugawa and Watari by 0.46, 0.76, 1.49, 1.55, and 0.26°C, respectively, compared to those in Sendai City. At 1300 JST, the temperature difference between Sendai City and these five stations are between 0.15 and 1.04°C. In February, at 0600 JST, the observed surface air temperatures at these same five stations decrease by 0.73, 0.75, 1.67, 1.65, and 0.23°C compared to that in Sendai City, whereas, at 1400 JST, these differences are between 0.31 and 1.10°C (Fig. 6). These results indicate that, at Sendai City, when the urban fractions decrease from a high value to a low residential area for one of the five other stations, the observed surface air temperatures at the five stations tend to decrease. An exception is Watari, showing that the result depends on geographical conditions.

Moreover, Figs. 7 and 8 show the August and February horizontal surface air temperature distribution between the OBS and the WRF data at 0500 and 1400 JST for the 2000s case. The WRF model can reproduce the horizontal temperature distribution in Sendai City and its surrounding area. The results between OBS and WRF data from both urban and non-urban stations show similar negative biases for the wide

Table 3. Mean bias and correlation coefficient (R) between simulated and observed daily surface air temperatures in August and February for 2000–2009.

Index	Station name	Land-use (LU) category	Long	Lat	Bias August	R August	Bias February	R February
1	Sendai	High residential/Commercial (HR)	140.89	38.26	−0.31	0.98	−0.93	0.98
2	Ishinomaki	High residential/Commercial (HR)	141.29	38.42	−0.45	0.99	−0.44	0.99
3	Shiogama	Medium residential (MR)	141.02	38.32	−0.29	0.99	−0.77	0.99
4	Kesennuma	Medium residential (MR)	141.55	38.90	−0.72	0.99	−1.17	0.98
5	Shizugawa	Low residential (LR)	141.44	38.68	−0.47	0.99	−1.50	0.97
6	Watari	Low residential (LR)	140.85	38.02	−1.18	0.99	−1.12	0.99

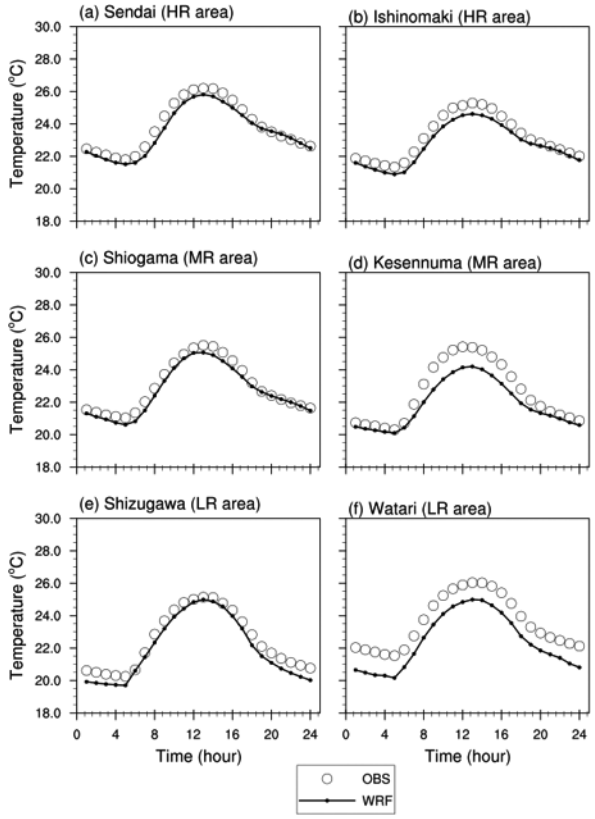

Fig. 5. August mean (2000–2009) surface air temperature variation for (a) Sendai City, (b) Ishinomaki, (c) Shiogama, (d) Kesennuma, (e) Shizugawa, and (f) Watari. The solid line is simulation (WRF) and the open circles are observations (OBS).

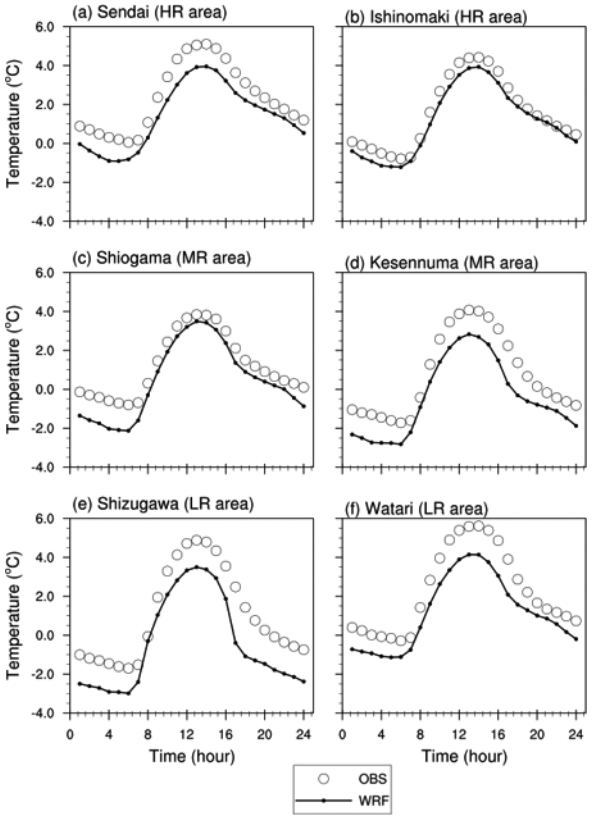

Fig. 6. Same details as that in Fig. 5, but for the month of February.

domain. To evaluate the UHI effect, the biases must cancel as we have focused on UHI and the impact of urbanization on the surface air temperature because of the land-use changes and AH releases between the PNV, LU1850s, 1850s, LU2000s, and 2000s cases.

In the 2000s case, the results from the OBS and WRF data for August show that the surface air temperatures are higher at 0500 JST and lower at 1400 JST near the coastline (Fig. 7). However, in February, both at 0500 and 1400 JST (Fig. 8), a higher surface air temperature is observed close to the coastline compared to the other area. Important influences on the surface air temperature distribution in and around Sendai City are the radiation, land surface heating, and surface wind. In Section 4, the impact of radiation and land surface heating will be discussed, and the effect of surface wind will be discussed later.

b. Surface wind

Because Sendai City is located close to the Pacific Ocean, sea breeze has an impact on the variation of the surface air temperature in summer. Generally, in winter, a northwesterly wind is observed. The development of sea breeze increases the wind speed, particularly near the coastline. We identified that the WRF model tends to overestimate the wind speed, particularly in August at 1400 JST (Fig. 9d). However, the model can reproduce the horizontal wind distribution and the influence of sea breeze.

During August, at 0500 JST (Figs. 9a, b), the wind in Sendai City was weak and the surface air temperature gradually increased toward the coastline (Figs. 7a, b). The wind speeds in the 2000s, 1850s, and PNV cases were 0.10, 0.54, and 0.56 m s^{-1}, respectively, at the central part of Sendai City (not shown). The southeasterly wind from ocean to land occurs at 1400 JST (Figs. 9c, d), indicating that the sea breeze might cool the surface air temperature over the target regions along the coastline. The results show that, at the cen-

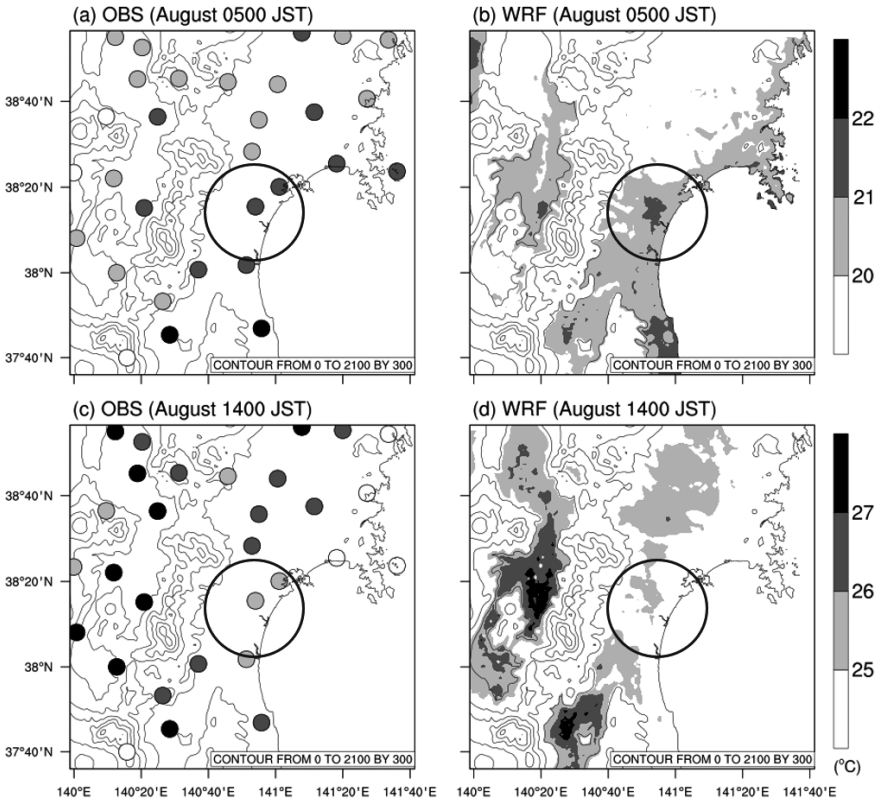

Fig. 7. August mean (2000–2009) distributions of surface air temperature from observations (OBS) and simulations (WRF) for the 2000s land-use case. (a) OBS data at 0500 JST, (b) WRF data at 0500 JST, (c) OBS data at 1400 JST, and (d) WRF data at 1400 JST. The big open circle represents Sendai City and its surrounding suburbs. The mean temperatures over the ocean area are masked out.

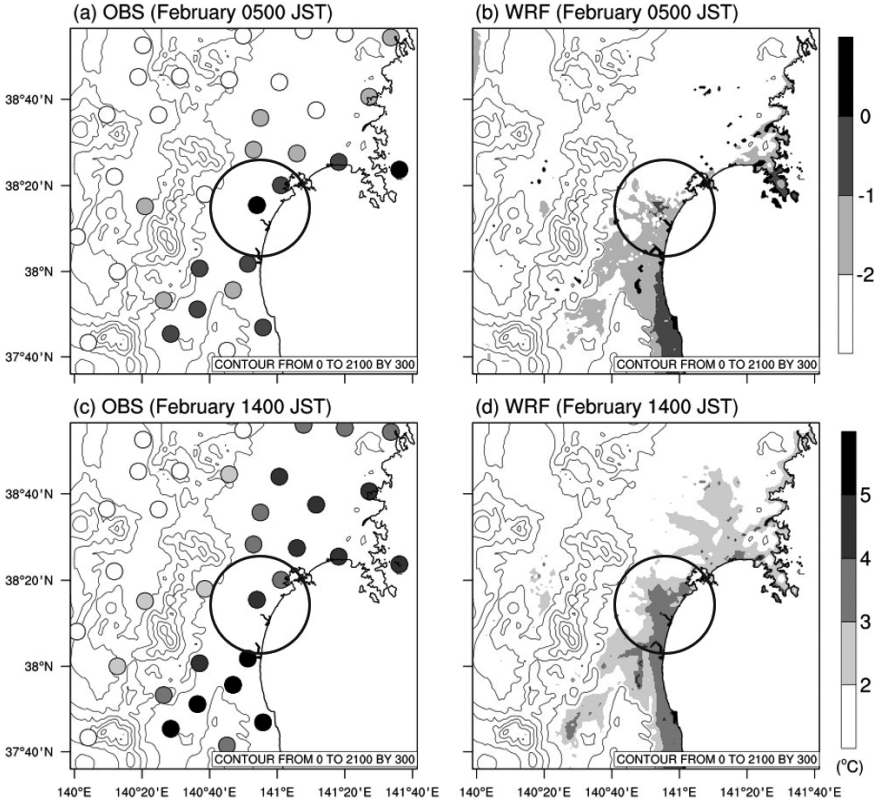

Fig. 8. Same details as that in Fig. 7, but for the month of February.

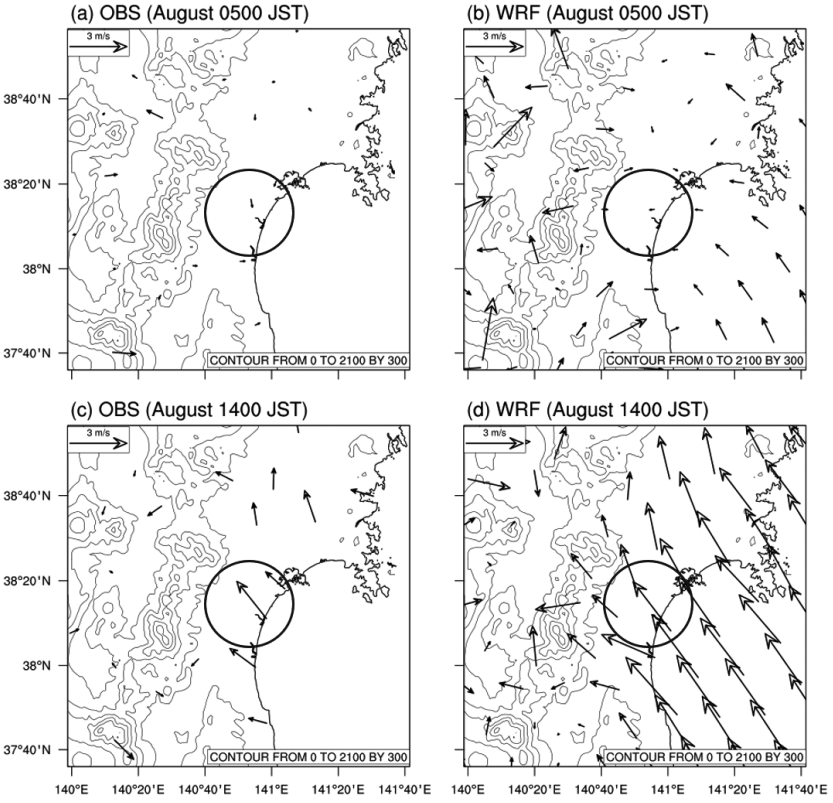

Fig. 9. August mean (2000–2009) wind distribution from observations (OBS) and simulations (WRF) for the 2000s land-use case. (a) OBS data at 0500 JST, (b) WRF data at 0500 JST, (c) OBS data at 1400 JST, and (d) WRF data at 1400 JST. The big open circle represents Sendai City and its surrounding suburbs.

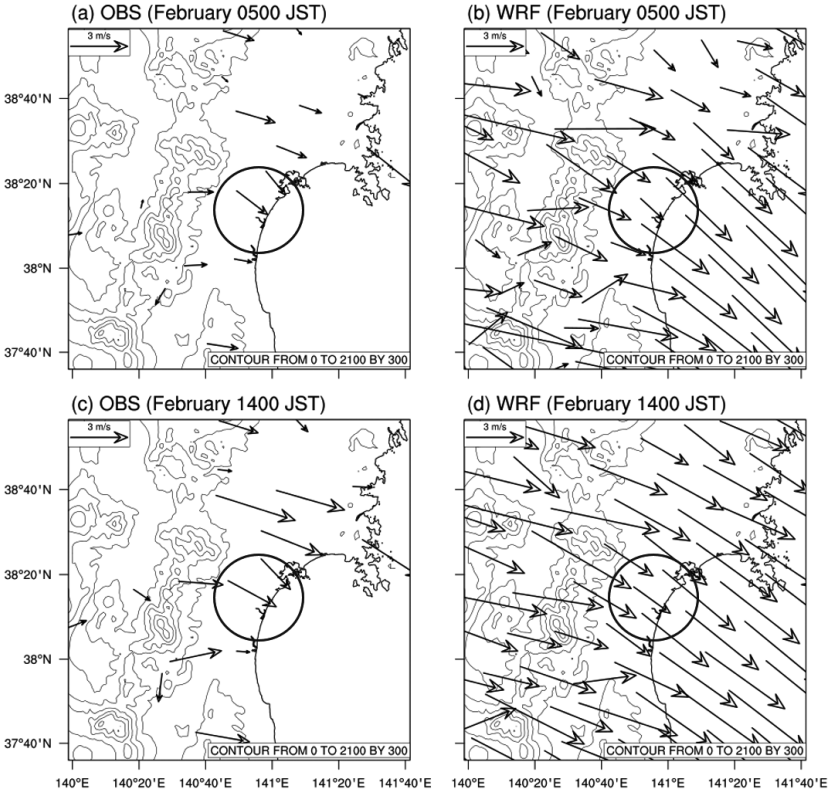

Fig. 10. Same details as that in Fig. 9, but for the month of February.

tral part of Sendai City, the sea breeze in 2000s case (2.26 m s^{-1}) slows by 0.56 and 1.03 m s^{-1} compared to the 1850s and PNV cases, respectively (not shown). In February, the strong northwesterly wind approaches Sendai City (Fig. 10). At 0500 and 1400 JST, the wind speeds at the central part of Sendai City in the 2000s case are 1.38 and 2.25 m s^{-1}, respectively. The wind in the 2000s case at 0500 and 1400 JST slows down by 0.59 and 0.47 m s^{-1}, respectively, compared to the 1850s case; however, when compared to the PNV case, it slows down by 0.84 and 0.78 m s^{-1}, respectively (not shown). The above mentioned results indicate that the wind in the 2000s case in August and February at 0500 and 1400 JST slows down compared to that in the 1850s and PNV cases. For the 2000s case, the surface roughness increases associated with urbanization in Sendai City would cause the wind speed decreases in the urban area.

3.3 *The impact of historical land-use changes and AH release*

First, we estimated the overall impact of urbanization in Sendai City, i.e., land-use changes and AH release. For this purpose, we compared the surface air temperature distributions between the PNV and 1850s and between the 1850s and 2000s cases. The experiments using the PNV and 1850s land-use data show slight temperature differences between the two cases at 0500 and 1400 JST in August and February (Figs. 11a, c, 12a, c). However, there were significant

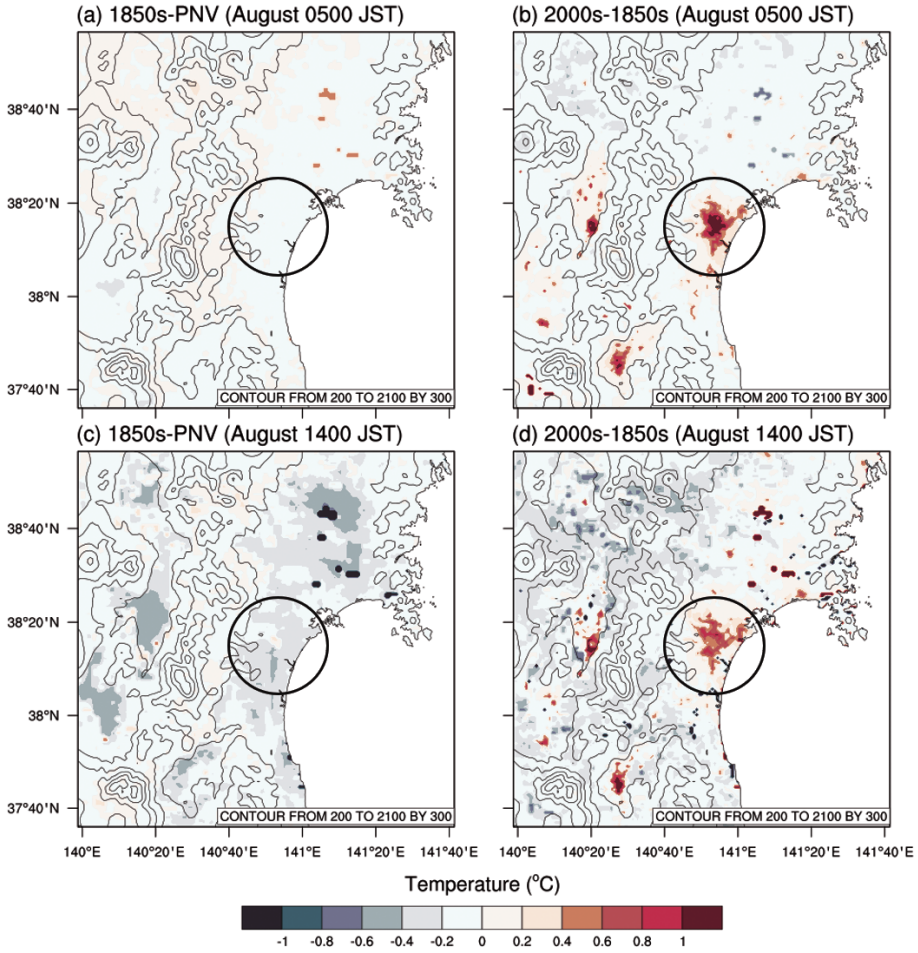

Fig. 11. August mean (2000–2009) change in surface air temperatures between (a) the PNV and 1850s cases at 0500 JST, (b) the 1850s and 2000s cases at 0500 JST, (c) the PNV and 1850s cases at 1400 JST, and (d) the 1850s and 2000s cases at 1400 JST. The big open circle is the same as in previous figures. The mean temperatures over the ocean area are masked out.

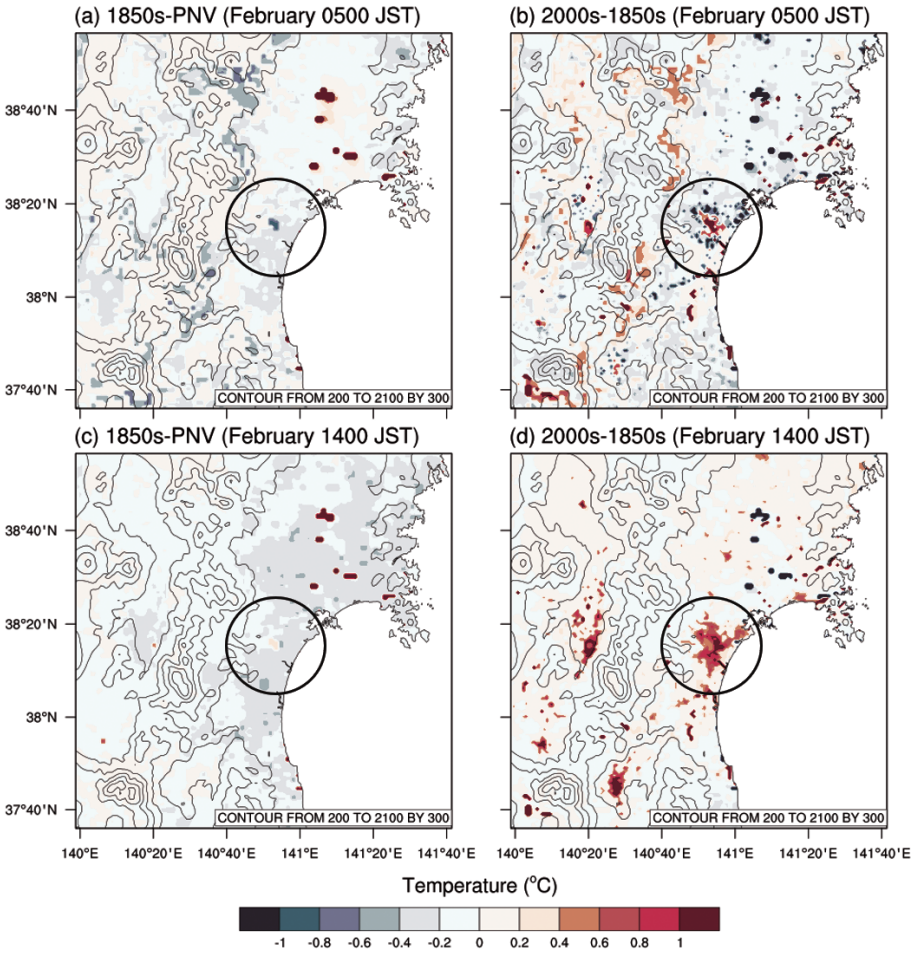

Fig. 12. Same details as that in Fig. 11, but for the month of February.

increases in the surface air temperatures occur in the 2000s (Figs. 11b, d, 12b, d). The current monthly mean temperature for central Sendai City is over 1.00°C higher than that in the 1850s. Moreover, we considered the diurnal variation of the surface air temperature at CCS in Sendai City, the TCA of Sendai City, and the green point near Sendai City (Fig. 13). In August, the surface air temperatures in the PNV case slightly increased (0.10–0.30°C) during the day and at night compared to that in 1850s case for CCS and TCA (Figs. 13a, c, Table 4). In particular, in February for CCS, the temperature in the PNV at night is higher (0.80°C) than that in the 1850s case (Fig. 13b). The reasons for this temperature increase in the 1850s case will be discussed in detail in Section 4. Meanwhile, compared to the 1850s, the results obtained from the 2000s for CCS show considerable nocturnal temperature increases of 2.00°C in August and 2.20°C in February (Figs. 13a, b, Table 4). This difference decreases during the day to 0.60°C in August and 0.80°C in February. However, for TCA (Figs. 13c, d), which includes central and suburban areas, the temperature differences between the 2000s and the 1850s cases are less than at CCS because of the reduced urban fraction and AH releases. For TCA, the temperature differences between the 2000s and 1850s cases are 0.80 and 0.30°C at night; however, during the day, they are 0.40°C in August and 0.30°C in February (Table 4). In the green point (Figs. 13e, f), all land-use cases have approximately the same temperatures. These results indicate that the impact of the urban-type change from 1850 to 2000 on the surface air temperature exceeds that of the land-use change from cropland (forest) to urban areas for both CCS and TCA. Indeed, when we compare the mean surface air temperature differences amongst all cases, at 0500 and 1400 JST, the most

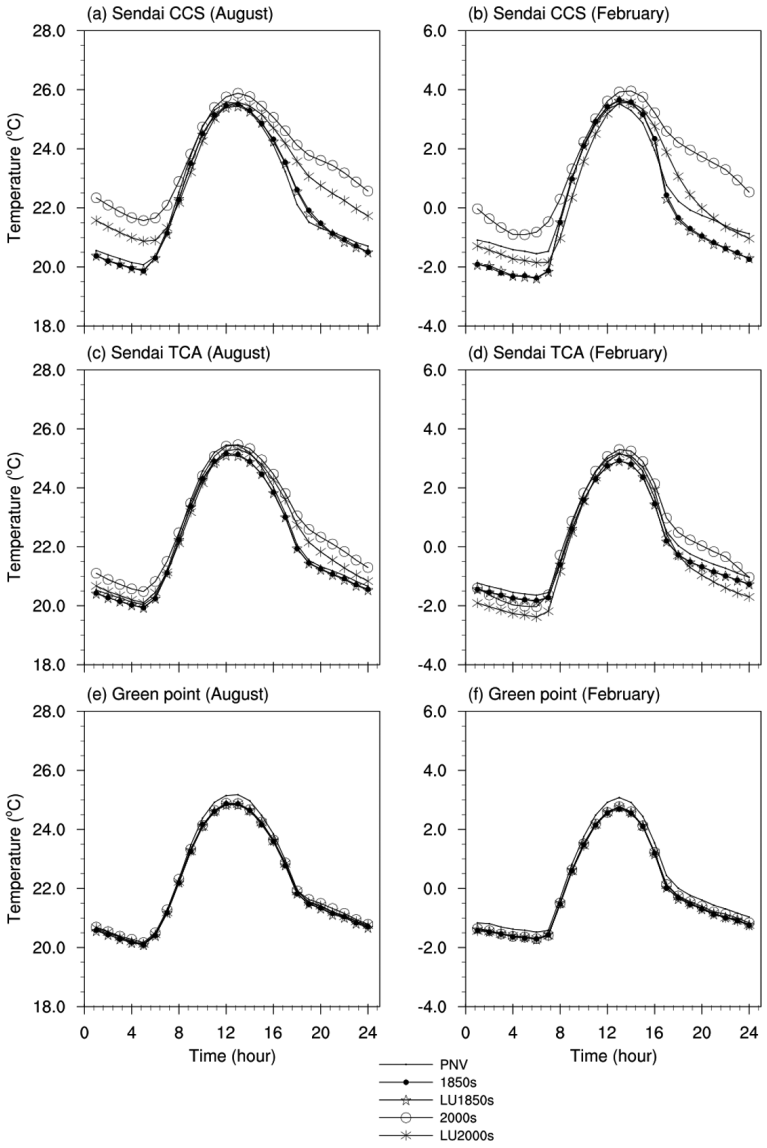

Fig. 13. Simulated monthly mean (2000–2009) diurnal surface air temperature variations in Sendai City. (a) At CCS in August. (b) At CCS in February. (c) For the total city area (TCA) in August. (d) TCA in February. (e) At the green point in August. (f) At green point in February. The location of the green point is shown in Fig. 1b. Legend is shown at the bottom.

Table 4. Simulated monthly mean (2000–2009) surface air temperatures in August and February at CCS and TCA in Sendai City during the day (0600–1700 JST) and at night (1800–0500 JST).

Period	August (CCS)		February (CCS)		August (TCA)		February (TCA)	
	Day	Night	Day	Night	Day	Night	Day	Night
PNV	23.9	20.8	1.5	−0.8	23.8	20.8	1.3	−0.9
1850s	23.8	20.8	1.4	−1.6	23.5	20.7	1.1	−1.2
2000s	24.4	22.8	2.2	0.6	23.9	21.5	1.4	−0.9
LU2000s	23.9	21.9	1.5	−0.8	23.7	21.1	1.1	−1.5

significant increases in the temperature occur between the 2000s and 1850s cases (Fig. 14).

The results show that the 2000s' monthly mean surface air temperatures for the CCS of Sendai City are higher than those in the 1850s by 1.30°C for August and 1.40°C for February (Figs. 14a, b). At 0500 JST (Figs. 14c, d), the temperatures between the 2000s and 1850s cases are 1.71°C in August and 1.39°C in February; however, at 1400 JST (Figs. 14e, f), these values are only ~0.40°C for both months. Furthermore, almost all results show that the temperatures between the 2000s and 1850s cases for CCS are higher than those for TCA. The reason for the temperature increases in the 2000s between CCS and TCA will be discussed in Section 4.

Second, a comparison between the 1850s and LU2000s cases indicates the impact of land-use changes during the past 150 years in Sendai City. Because of the similarity of the 1850s and PNV cases, we do not consider the latter here. For CCS in August, Fig. 13a and Table 4 show that the mean surface air temperatures between the 1850s and LU2000s cases increase by 0.10°C during the day and 1.10°C at night, whereas, in February, these differences are 0.80 and 0.10°C (Fig. 13b, Table 4), respectively. For TCA in August, these surface air temperature differences are 0.40°C at night and 0.20°C during the day, whereas in February, the difference is only 0.30°C during the day (Figs. 13c, d, Table 4). When we compare the daily mean surface air temperatures at 0500 and 1400 JST between the 1850s and LU2000s cases, a significant temperature difference of 1.04°C occurs for CCS in August at 0500 JST (Fig. 14c). In February, this difference is 0.50°C (Fig. 14d). At 1400 JST, the results in August and February at CCS show that the surface air temperatures increase by 0.20 and 0.02°C, respectively, whereas, for TCA, the temperature differences are around 0.30°C for both cases (Figs. 14e, f).

Third, to estimate the impact of AH release in Sendai City, we compare the mean diurnal surface air temperatures between the LU1850s and 1850s and between the LU2000s and 2000s (Fig. 13, Table 4). The results between the LU1850s and 1850s cases show a small temperature difference for both months (0.10°C), indicating a negligible effect of AH in the 1850s. Moreover, we simulated monthly mean surface air temperatures between the LU2000s and 2000s cases for Sendai City. The results in August for CCS show that surface air temperatures increase by 0.90°C at night and 0.50°C during the day (Fig. 13a). In February, the surface air temperatures increased because of AH release by 1.40°C at night and 0.70°C during the day (Fig. 13b). These results show that the impact of the AH release in August is lesser than that of land-use changes in Sendai City at night but higher during the day. However, in February, the impact of AH release dominates over that of land-use changes. The warming effect in February is because of the relatively large energy consumption, which contributes to a large sensible heat. Aoyagi et al. (2012) and Ma et al. (2017) found a similar contribution between AH release and land-use changes. For TCA (Fig. 13c), the surface air temperatures between the LU2000s and 2000s cases in August are 0.40°C at night and 0.30°C during the day. However, in February (Fig. 13d), the differences between the LU2000s and 2000s cases are 0.60°C at night and 0.30°C during the day (Table 4). These results show that, in August, the impact of the AH release for TCA is equal to that of land-use changes, whereas, in February, the surface air temperatures rises primarily because of the impact of AH release. According to Figs. 14a and 14b, the daily mean surface air temperatures in the 2000s case in August and February increase by 0.70 and 1.00°C for CCS and by 0.30 and 0.50°C for TCA compared to those for the LU2000s case. At 0500 JST in August and February, these increases are 0.67 and 0.89°C for CCS and by 0.38 and 0.29°C for TCA (Figs. 14c, d). At 1400 JST, the surface air temperatures in the 2000s case increase over those in the LU2000s case by 0.27 and 0.36°C for CCS and by 0.13 and 0.15°C for TCA, in August and February, respectively (Figs. 14e, f).

We also estimated the impact of land-use changes and AH releases between the PNV and 1850s and between the 1850s and 2000s for Ishinomaki, Shiogama, Kesennuma, Shizugawa, and Watari (Fig. 15). The results show that the surface air temperature differences between the PNV and 1850s are between 0.10 and 0.30°C for both August and February for all stations. However, in August, for the 2000s case, we identified a significant temperature increase over that in the 1850s in Ishinomaki. At night, the increase is 1.30°C but 0.40°C during the day, whereas, in February, these increases are 1.00 and 0.50°C.

An interesting aspect here is about the surface air temperatures in the 2000s in February in Shiogama and Kesennuma (Shizugawa and Watari), which are lower than those in the PNV and the 1850s case from midnight to early morning (evening to early morning). The lower temperature is because of the forest canopy in the PNV case producing a smaller radiative cooling compared to the grasslands in the 2000s case. For the urban grid in the 2000s case, the grid cell, except for the urban fraction, is covered by grasslands in the

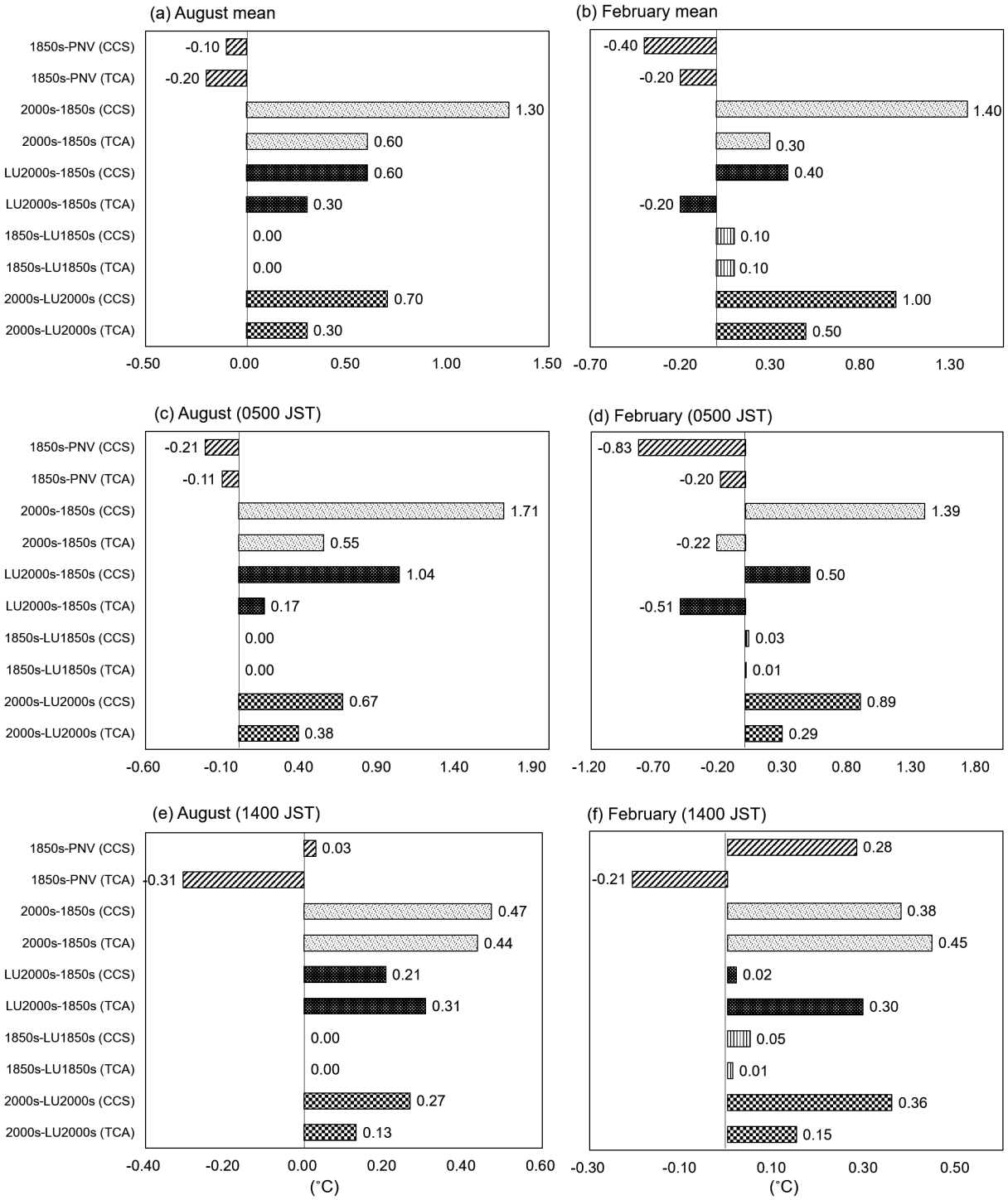

Fig. 14. Differences in monthly mean surface air temperatures between simulation cases. (a) Daily mean in August. (b) Daily mean in February. (c) At 0500 JST in August. (d) At 0500 JST in February. (e) At 1400 JST in August. (f) At 1400 JST in February.

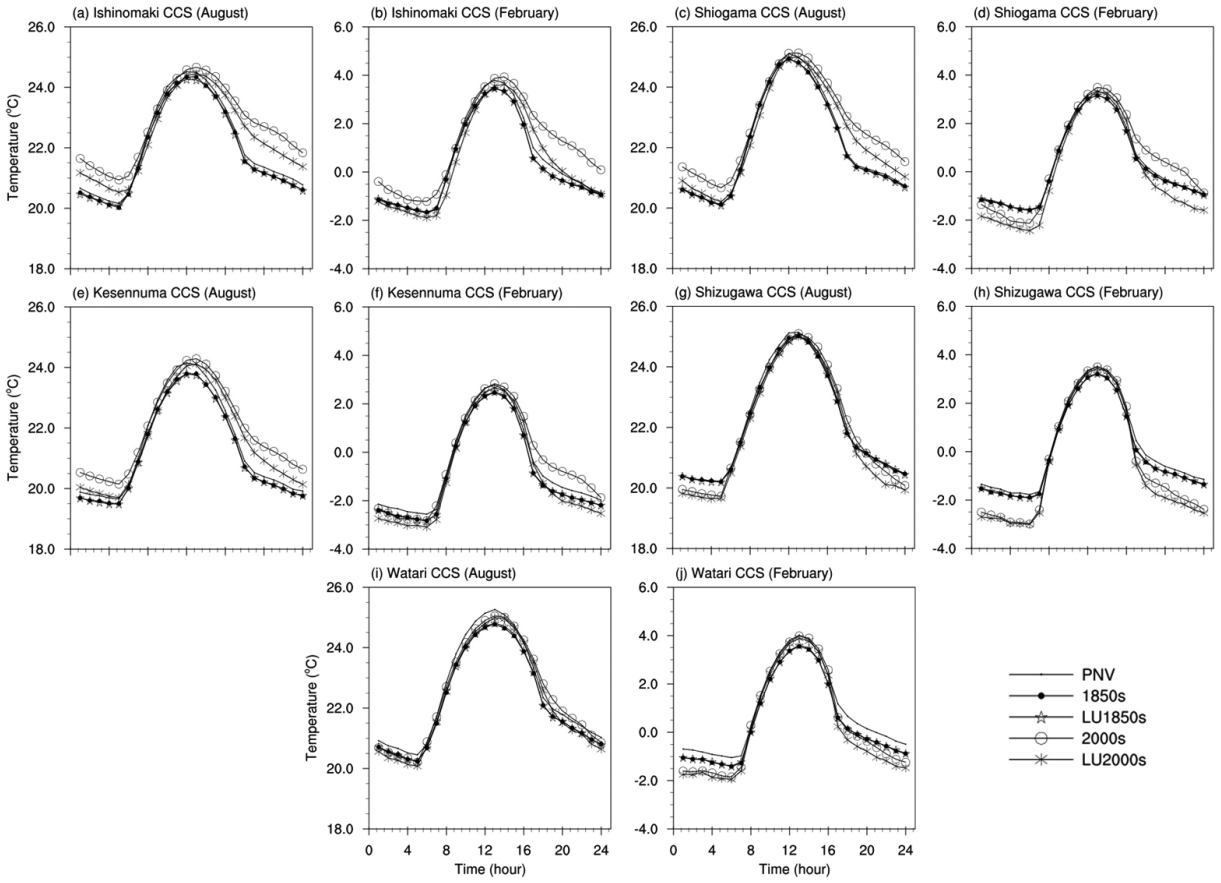

Fig. 15. Simulated monthly mean (2000–2009) diurnal surface air temperature variations for surrounding sites.

Noah-LSM model coupled with UCM. Moreover, because of the drier surface in the 2000s (Figs. 16k, n), the thermal inertia is smaller than that for the PNV and the 1850s case. Another reason for the lower surface air temperature in the 2000s case is that the AH release is insufficient to offset the increase in radiative cooling and smaller thermal inertia over the area with a small urban fraction. These results indicate that the impact of the land-use changes and AH release significantly increase the surface air temperatures in Sendai City and Ishinomaki, which belong to the HR area, whereas the impact is lesser for less-urbanized cities such as Shiogama, Kesennuma, Shizugawa, and Watari, which belong to the MR and LR areas.

4. Discussion

First, we examined the causes of the nocturnal temperature difference between the PNV and 1850s cases as described in Subsection 3.3. Figure 17 shows the monthly mean vertical profiles of potential temperatures for CCS in August and February at 0500 JST for all cases. If we consider the potential temperature for the PNV and the 1850s cases near the surface, the nocturnal boundary layers of the PNV and 1850s cases are stable in August with nearly equal potential temperatures near the surface (Fig. 17a). However, in February, the potential nocturnal temperature near the surface for the PNV case is higher than that for the 1850s case (Fig. 17b). Moreover, this difference is seen in Fig. 13b. To understand the cause for such difference, we examined the diurnal variations of the surface heat budget terms (Figs. 18, 19, Tables 5, 6), which show that the sensible heat (SH) and ground heat (GH) at night in the PNV and 1850s cases are nearly the same. However, the net radiation (Rn) in the PNV case at night is 8.70 W m^{-2} higher than that in the 1850s case because of the larger upward longwave radiation for PNV (296.83 W m^{-2}) compared to that in the 1850s case (288.57 W m^{-2}). These results indicate that the radiative cooling for the PNV case

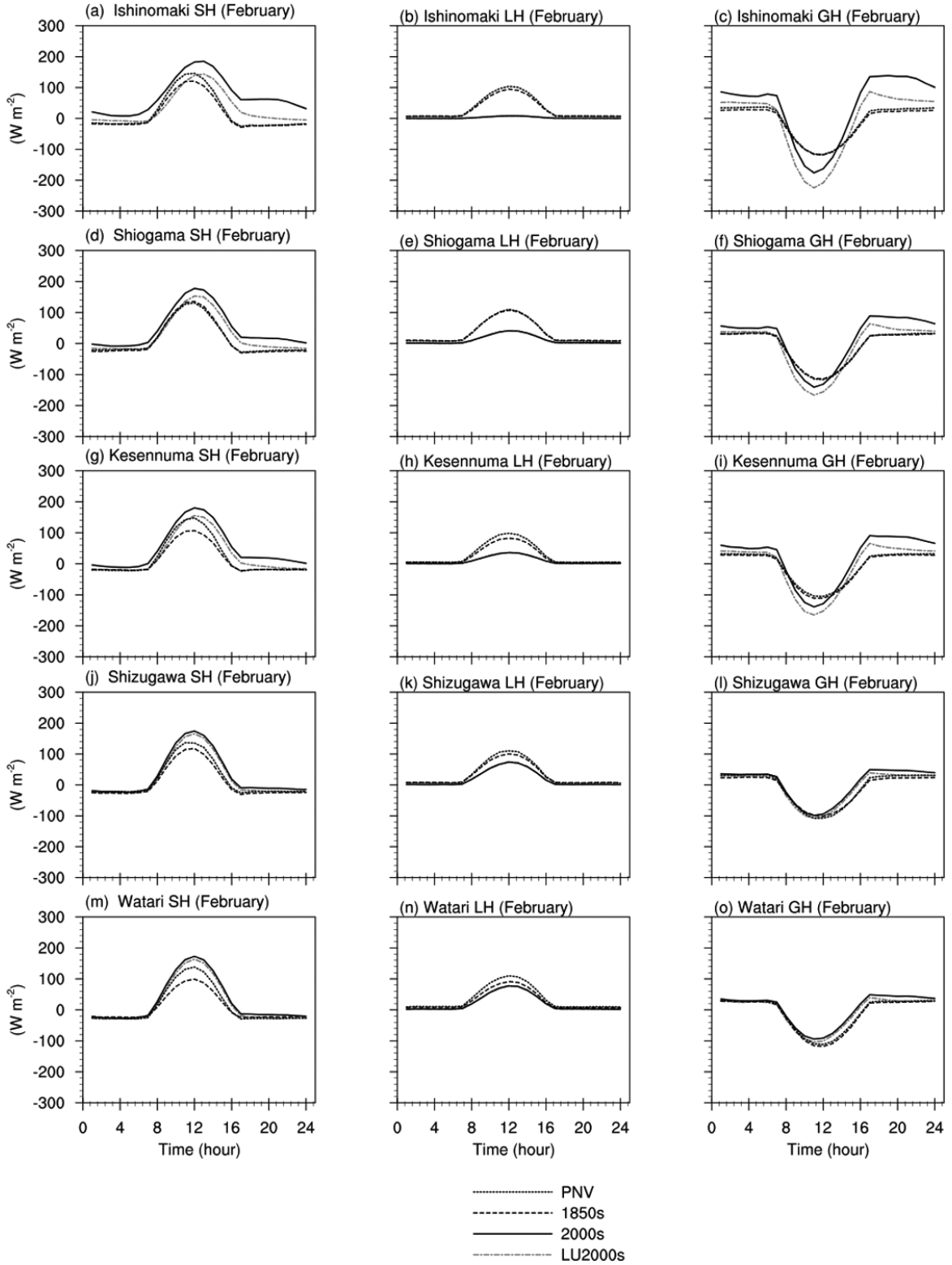

Fig. 16. Monthly mean (2000–2009) diurnal variations of surface heat fluxes at the surrounding sites from the WRF model in February. Legend is shown at the bottom.

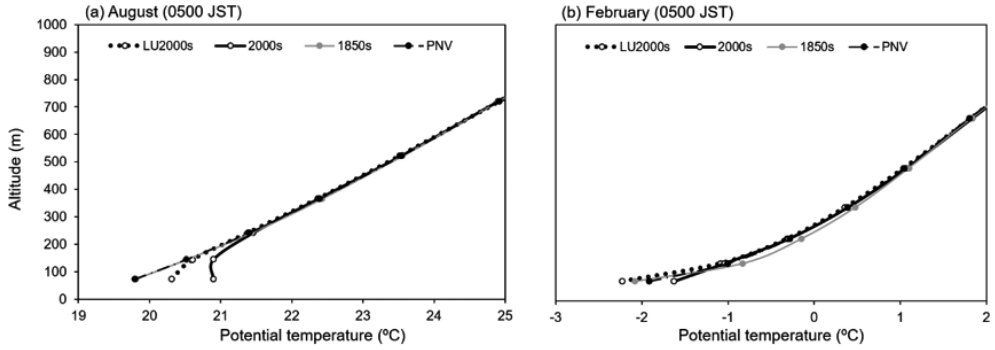

Fig. 17. Vertical profiles of potential temperature at 0500 JST at Sendai City from the WRF model for four land-use cases. (a) August. (b) February.

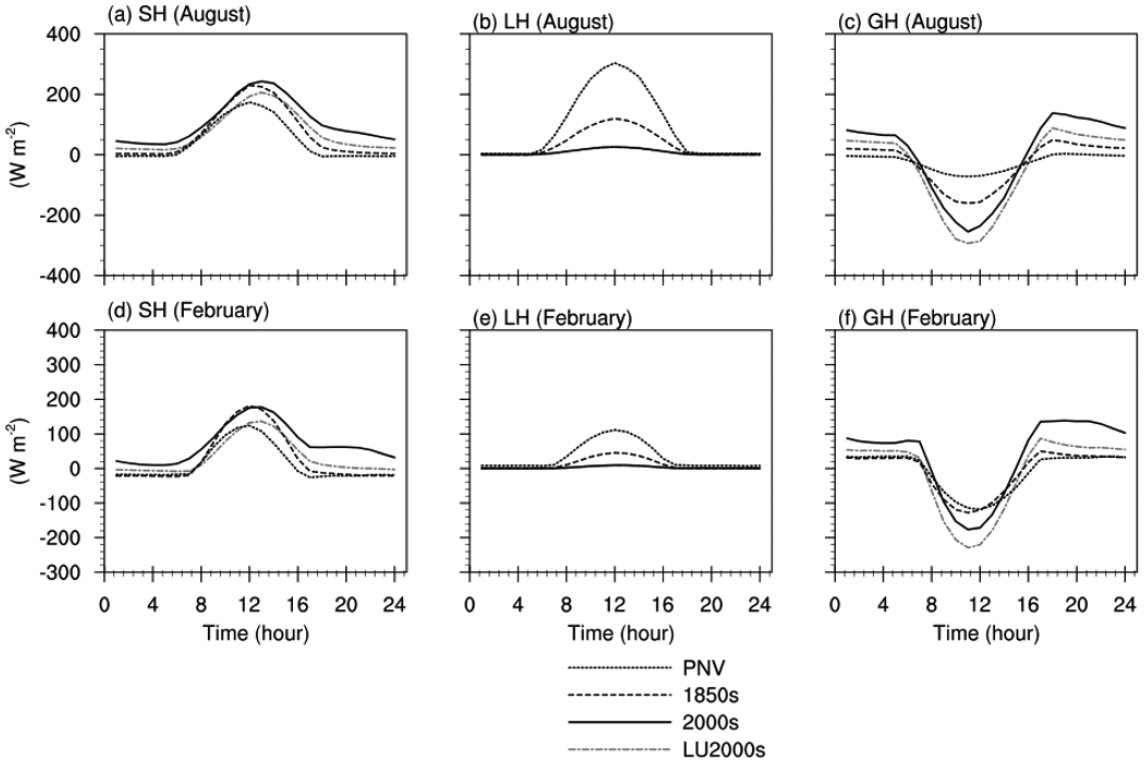

Fig. 18. Monthly mean (2000–2009) diurnal variations of surface heat fluxes in Sendai City at CCS from the WRF model.

is smaller than that in the 1850s case. One reason for lesser radiative cooling in the PNV case is probably the forest canopy effect. Another reason is that, for the 1850s case, the dry, sparse wooden buildings and small urban fraction led to stronger radiation cooling. Moreover, the difference in downward longwave radiation between the PNV (244.78 W m^{-2}) and 1850s cases (244.32 W m^{-2}) at night was insignificant, suggesting negligible cloud-cover change for both cases in February.

Second, we studied the difference in the surface heat budget terms between CCS and TCA in Sendai City for February in the 2000s. We selected the 2000s case because it showed the largest difference in heat

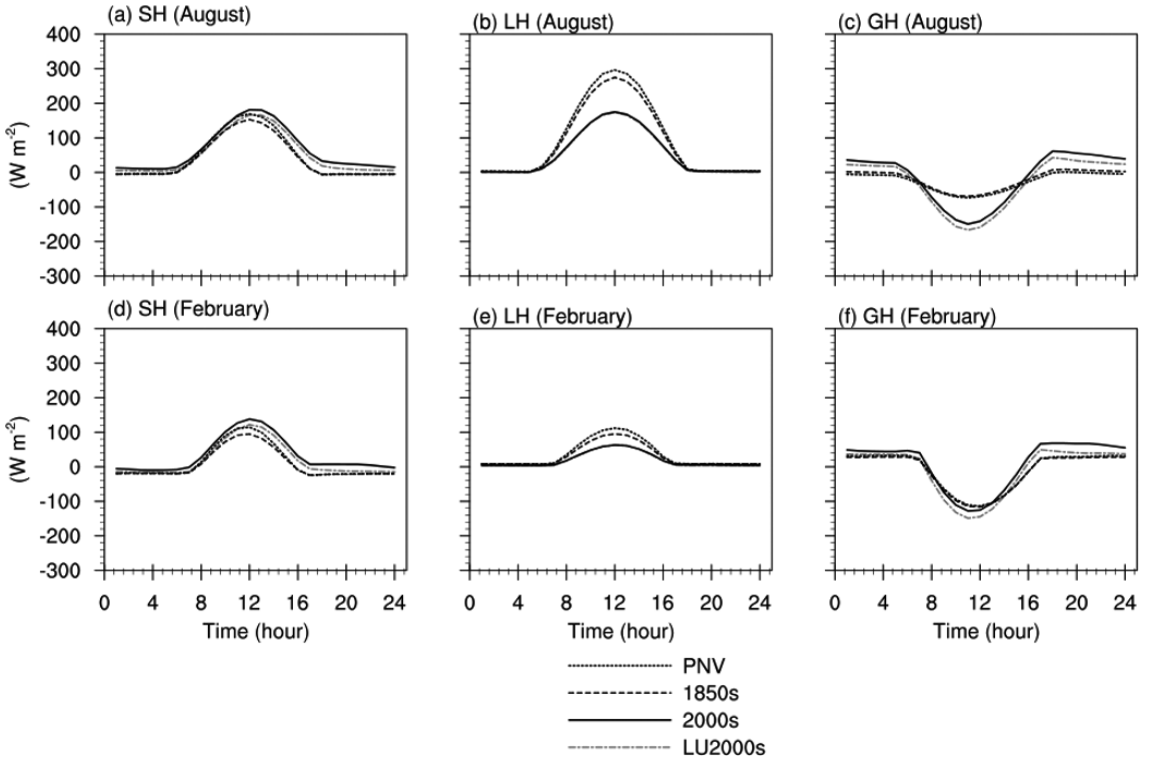

Fig. 19. Same details as that in Fig. 18, but for the TCA.

budget between CCS and TCA. For CCS, the LH flux was lesser during the day because of the high urban fraction in the HR area (Fig. 18e). Moreover, because of the high thermal inertia of the urban structures, the GH was high at night, and there was more outgoing radiation, which contributed to CCS having a higher nocturnal surface air temperature compared to TCA (Figs. 18f, 13b). However, for TCA, the small urban fraction is the reason for the increase in surface evaporation and LH flux during the day (Fig. 19e). Moreover, because of the small thermal inertia of the urban structures in TCA (HR + MR + LR), the GH at night is 50 % lesser than that for CCS (Figs. 18f, 19f, Tables 5, 6). Additionally, the relatively low AH release for TCA contributes to the relatively low SH flux at night compared to that for CCS (Figs. 18d, 19d, Tables 5, 6). As a result, the nocturnal surface air temperature for TCA is 1.50°C lower than that for CCS (Table 4). In August, a comparison of surface heat budget terms between CCS and TCA in the 2000s case indicates a similar result to that in February.

We have not evaluated the influence of snow cover on surface air temperature because the WRF/UCM models cannot evaluate effects of snow on temperature in urban areas. Moreover, this study focuses on the effect of land-use changes and AH releases on air temperature in Sendai City. Mori and Sato (2015) and Sugimoto et al. (2015b) investigated the effect of snow cover on the air temperature and the impact of land-use change on winter precipitation in Hokkaido, Japan. They identified that snow cover in the urban canopy layer reduced both the surface air temperature and effect of UHI, as well as led to a decrease in precipitation over the deforested areas between 1850 and 1985. The estimation of the influence of snow cover on the UHI and impact of urbanization in Sendai City will be the subject for a future study.

5. Conclusions

We examined the impact of urbanization on surface air temperature and UHI in Sendai City over the past 150 years using a WRF model with a 1-km horizontal grid spacing. We examined three experimental cases: one of PNV and two for realistic land-use (the 1850s and 2000s cases). The results are summarized as follows.

(1) The WRF model reproduced the observed surface air temperatures in the 2000s land-use case

Table 5. Simulated monthly mean (2000–2009) sensible heat (SH), latent heat (LH), ground heat (GH) fluxes, and net radiation (Rn) in August and February at CCS in Sendai City during the day (0600–1700 JST) and at night (1800–0500 JST).

CCS	August							
	Rn		SH		LH		GH	
Period	Day	Night	Day	Night	Day	Night	Day	Night
PNV	324.0	4.3	92.7	−3.9	181.2	2.9	−50.1	−5.3
1850s	284.5	−15.9	126.9	7.3	69.4	0.6	−88.2	23.8
2000s	274.7	−35.3	153.9	61.8	15.4	0.8	−105.5	94.4
LU2000s	286.9	−27.5	123.7	27.6	15.2	0.6	−147.9	55.6
CCS	February							
	Rn		SH		LH		GH	
Period	Day	Night	Day	Night	Day	Night	Day	Night
PNV	149.8	−41.9	41.2	−20.8	63.2	9.4	−45.4	30.5
1850s	144.5	−50.6	74.9	−20.1	24.6	1.6	−45.0	32.0
2000s	144.0	−68.3	104.8	36.7	5.5	0.9	−33.8	106.0
LU2000s	153.9	−58.9	65.0	−0.7	4.9	0.3	−83.9	58.4

Table 6. Simulated monthly mean (2000–2009) sensible heat (SH), latent heat (LH), ground heat (GH) fluxes, and net radiation (Rn) in August and February in TCA in Sendai City during the day (0600–1700 JST) and at night (1800–0500 JST).

TCA	August							
	Rn		SH		LH		GH	
Period	Day	Night	Day	Night	Day	Night	Day	Night
PNV	319.9	5.2	90.8	−4.6	178.2	2.9	−50.9	−6.9
1850s	286.5	−3.1	79.6	−4.4	161.5	1.9	−45.4	0.5
2000s	283.7	−19.8	107.5	18.5	103.5	2.0	−72.8	40.2
LU2000s	287.5	−17.2	97.3	7.8	103.4	1.9	−86.7	26.9
TCA	February							
	Rn		SH		LH		GH	
Period	Day	Night	Day	Night	Day	Night	Day	Night
PNV	144.5	−40.5	36.4	−21.9	63.7	9.9	−44.4	28.5
1850s	129.5	−37.7	28.1	−21.9	54.2	9.4	−47.1	25.2
2000s	134.4	−51.2	62.5	−1.7	36.0	5.7	−35.9	55.2
LU2000s	142.1	−48.2	51.3	−13.4	33.2	4.1	−57.5	38.8

for Sendai City and five stations in the surroundings reasonably well. The model mean biases of the surface air temperature ranged from −0.29 to −1.18°C in August and from −0.44 to −1.50°C in February.

(2) The sensitivity experiment between PNV and 1850s land-use cases showed that the monthly mean surface air temperatures for PNV were higher than those in the 1850s by 0.10°C in August and 0.40°C in February for CCS and by 0.20°C in both months for TCA.

(3) Between the 1850s and 2000s land-use cases in Sendai City, the simulated monthly mean surface air temperatures in the 2000s at CCS were higher than those in the 1850s by 1.30°C in August and 1.40°C in February, whereas, in TCA, the corresponding increases were 0.60 and 0.30°C.

(4) The simulated monthly mean surface air temperatures during the day (0600–1700 JST) and at night (1800–0500 JST) were examined in Sendai City. The results showed a significant nocturnal temperature

increase of 2.00°C in August and 2.20°C in February at CCS of Sendai City because of urbanization over the past 150 years (1850–2000). This difference decreased during the day to 0.60°C in August and 0.80°C in February.

However, for TCA, which includes suburban areas, the surface air temperature differences between the 2000s and 1850s land-use cases were less than those for CCS. At night, for TCA, the temperature between the 2000s and 1850s land-use cases were 0.80°C in August and 0.30°C in February. During the day, the corresponding values were 0.40 and 0.30°C.

(5) A comparison between the 1850s and LU2000s land-use cases showed the impact of land-use changes during the past 150 years in Sendai City. For CCS, in August, the mean surface air temperatures increased by 1.10°C at night and 0.10°C during the day, whereas, in February, these differences were 0.80 and 0.10°C.

For TCA, the surface air temperature increased between the 1850s and LU2000s land-use cases by 0.40°C both at night and during the day in August, whereas, in February, this difference was 0.30°C but only during the day.

(6) To estimate the impact of AH releases in Sendai City, we examined the mean diurnal surface air temperatures between the LU1850s and 1850s and between the LU2000s and 2000s. The results between the LU1850s and 1850s land-use cases demonstrated only a small temperature difference for both August and February (0.10°C). Furthermore, the effect of AH in the 1850s land-use case was negligible. The simulated monthly mean surface air temperatures between the LU2000s and 2000s land-use cases increased in August for CCS by 0.90°C at night and 0.50°C during the day. Comparing the 1850s and 2000s land-use cases, the results showed that the impact of AH release was lesser at night than that in the land-use changes in Sendai City; however, it was higher during the day. In February, the temperatures increased because of AH releases by 1.40°C at night and 0.70°C during the day. These results showed that, in February, the impact of AH releases was higher than that from land-use changes.

For TCA, in August, the surface air temperatures between the LU2000s and 2000s land-use cases were 0.40°C at night and 0.30°C during the day. The results indicated that the impact of AH release was the same as that for land-use changes. However, in February, a difference was found only between the LU2000s and 2000s land-use cases at night (0.60°C) and during the day (0.30°C). This indicates that for TCA, in February, the temperatures increased primarily because of the impact of AH release.

(7) The differences between the SH, LH, and GH heat fluxes in August and February for PNV, 1850s, LU2000s, and 2000s land-use cases were evaluated. The results indicated that in the 2000s for CCS, a reduction of LH during the day and a storage of GH at night helped increase the nocturnal surface air temperature in Sendai City. In the 2000s land-use case, these temperatures increased over those in the 1850s case by 2.00°C in August and 2.20°C in February. However, for TCA, the change in heat flux was less significant than that for CCS, making the corresponding nocturnal mean surface air temperatures change by 0.80 and 0.30°C.

Acknowledgments

We would like to thank the Tohoku Electric Company and Sendai City Gas for providing the essential data for this study. The past (1850) land-use information data in this study was created by Prof. Yukio Himiyama, Hokkaido University of Education, and Prof. Shoichiro Arizono, Aichi University. The data was provided from the book Atlas - Environmental Change in Modern Japan, Asakura Publishing Co., Ltd. Moreover, the present work was supported by the 'Interdisciplinary Computational Science Program' at the Center for Computational Sciences, the University of Tsukuba, and by the Social Implementation Program on Climate Change Adaptation Technology (SI-CAT) of the Ministry of Education, Culture, Sports, Science and Technology (MEXT).

References

Adachi, S. A., F. Kimura, H. Kusaka, T. Inoue, and H. Ueda, 2012: Comparison of the impact of global climate changes and urbanization on summertime future climate in the Tokyo metropolitan area. *J. Appl. Meteor. Climatol.*, **51**, 1441–1454.

Aizawa, E., 1892: *Eiri meisai Sendai shigai zenzu*. Stanford University Libraries. [Available at https://purl.stanford.edu/qb218dr9292.]

Aoyagi, T., N. Kayaba, and N. Seino, 2012: Numerical simulation of the surface air temperature change caused by increases of urban area, anthropogenic heat, and building aspect ratio in the Kanto-Koshin area. *J. Meteor. Soc. Japan*, **90B**, 11–31.

Argüeso, D., J. M. Hidalgo-Muñoz, S. R. Gámiz-Fortis, M. J. Esteban-Parra, and Y. Castro-Díez, 2012: High-resolution projections of mean and extreme precipitation over Spain using the WRF model (2070–2099 versus 1970–1999). *J. Geophys. Res.*, **117**, D12108, doi:10.1029/2011JD017399.

Argüeso, D., J. P. Evans, L. Fita, and K. J. Bormann, 2014:

Temperature response to future urbanization and climate change. *Climate Dyn.*, **42**, 2183–2199.

Arizono, S., 1995: 1.2 Land Use in Japan circa 1850. 1.3 Land Use in Japan circa 1900. *Atlas - Environmental Change in Modern Japan*. Himiyama, Y., I. Ohta, T. Tamura, T. Arai, and Y. Kubo (eds.), Asakura Publishing Co., Ltd., 4–5, 6–7 (in Japanese).

Bhati, S., and M. Mohan, 2016: WRF model evaluation for the urban heat island assessment under varying land use/land cover and reference site conditions. *Theor. Appl. Climatol.*, **126**, 385–400.

Chen, F., and J. Dudhia, 2001: Coupling an advanced land surface–hydrology model with the Penn State–NCAR MM5 modeling system. Part I: Model implementation and sensitivity. *Mon. Wea. Rev.*, **129**, 569–585.

Chen, F., H. Kusaka, R. Bornstein, J. Ching, C. S. B. Grimmond, S. Grossman-Clarke, T. Loridan, K. W. Manning, A. Martilli, S. Miao, D. Sailor, F. P. Salamanca, H. Taha, M. Tewari, X. Wang, A. A. Wyszogrodzki, and C. Zhang, 2011: The integrated WRF/urban modelling system: Development, evaluation, and applications to urban environmental problems. *Int. J. Climatol.*, **31**, 273–288.

Chen, L., and O. W. Frauenfeld, 2016: Impacts of urbanization on future climate in China. *Climate Dyn.*, **47**, 345–357.

Chen, L., M. Zhang, and Y. Wang, 2016: Model analysis of urbanization impacts on boundary layer meteorology under hot weather conditions: A case study of Nanjing, China. *Theor. Appl. Climatol.*, **125**, 713–728.

City of Yokohama, 2000: *Population news of major cities*. [Available at http://www.city.yokohama.lg.jp/ex/stat/jinko/city/0012-e.html.]

Cui, Y. Y., and B. De Foy, 2012: Seasonal variations of the urban heat island at the surface and the near-surface and reductions due to urban vegetation in Mexico City. *J. Appl. Meteor. Climatol.*, **51**, 855–868.

Doan, Q.-V., and H. Kusaka, 2015: Numerical study on regional climate change due to the rapid urbanization of greater Ho Chi Minh City's metropolitan area over the past 20 years. *Int. J. Climatol.*, **36**, 3633–3650.

Doan, Q.-V., H. Kusaka, and Q.-B. Ho, 2016: Impact of future urbanization on temperature and thermal comfort index in a developing tropical city: Ho Chi Minh City. *Urban Climate*, **17**, 20–31.

Dudhia, J., 1989: Numerical study of convection observed during the winter monsoon experiment using a mesoscale two-dimensional model. *J. Atmos. Sci.*, **46**, 3077–3107.

Feng, J.-M., Y.-L. Wang, Z.-G. Ma, and Y.-H. Liu, 2012: Simulating the regional impacts of urbanization and anthropogenic heat release on climate across China. *J. Climate*, **25**, 7187–7203.

Gartland, L., 2012: *Heat Islands: Understanding and Mitigating Heat in Urban Areas*. Earthcan, 208 pp.

Geographical Survey Institute, 1977: *The National Atlas of Japan*. Japan Map Center, 218 pp.

Georgescu, M., G. Miguez-Macho, L. T. Steyaert, and C. P. Weaver, 2009a: Climatic effects of 30 years of landscape change over the Greater Phoenix, Arizona, region: 1. Surface energy budget changes. *J. Geophys. Res.*, **114**, D05110, doi:10.1029/2008JD010745.

Georgescu, M., G. Miguez-Macho, L. T. Steyaert, and C. P. Weaver, 2009b: Climatic effects of 30 years of landscape change over the Greater Phoenix, Arizona, region: 2. Dynamical and thermodynamical response. *J. Geophys. Res.*, **114**, D05111, doi:10.1029/2008JD010762.

Georgescu, M., M. Moustaoui, A. Mahalov, and J. Dudhia, 2011: An alternative explanation of the semiarid urban area "oasis effect". *J. Geophys. Res.*, **116**, D24113, doi:10.1029/2011JD016720.

Giannaros, T. M., D. Melas, I. A. Daglis, I. Keramitsoglou, and K. Kourtidis, 2013: Numerical study of the urban heat island over Athens (Greece) with the WRF model. *Atmos. Environ.*, **73**, 103–111.

Grossman-Clarke, S., J. A. Zehnder, T. Loridan, and C. S. B. Grimmond, 2010: Contribution of land use changes to near-surface air air temperatures during recent summer extreme heat events in the Phoenix metropolitan area. *J. Appl. Meteor. Climatol.*, **49**, 1649–1664.

Hamdi, R., H. Van de Vyver, R. De Troch, and P. Termonia, 2014: Assessment of three dynamical urban climate downscaling methods: Brussels's future urban heat island under an A1B emission scenario. *Int. J. Climatol.*, **34**, 978–999.

Heaviside, C., X.-M. Cai, and S. Vardoulakis, 2015: The effects of horizontal advection on the urban heat island in Birmingham and the West Midlands, United Kingdom during a heatwave. *Quart. J. Roy. Meteor. Soc.*, **141**, 1429–1441.

Himiyama, Y., 1995: 1.1 Modernization and Land Use Change. *Atlas - Environmental Change in Modern Japan.* Himiyama, Y., I. Ohta, T. Tamura, T. Arai, and Y. Kubo (eds.), Asakura Publishing Co., Ltd., 2-3 (in Japanese).

Hong, S.-Y., J. Dudhia, and S.-H. Chen, 2004: A revised approach to ice microphysical processes for the bulk parameterization of clouds and precipitation. *Mon. Wea. Rev.*, **132**, 103–120.

Ichinose, T., 2003: Regional warming related to land use change during recent 135 years in Japan. *J. Global Environ. Eng.*, **9**, 19–40.

Iizuka, S., Y. Xuan, and Y. Kondo, 2015: Impacts of disaster mitigation/prevention urban structure models on future urban thermal environment. *Sustainable Cities. Soc.*, **19**, 414–420.

Janjić, Z. I., 1994: The step-mountain eta coordinate model: Further developments of the convection, viscous sublayer, and turbulence closure schemes. *Mon. Wea. Rev.*, **122**, 927–945.

Japan Meteorological Agency, 2016: *Sendai average value*

per year/month. [Available at http://www.data.jma.go.jp/obd/stats/etrn/view/nml_sfc_ym.php?prec_no=34&prec_ch=%8B%7B%8F%E9%8C%A7&block_no=47590&block_ch=%90%E5%91%E4&year=&month=&day=&elm=normal&view=.]

Kain, J. S., 2004: The Kain–Fritsch convective parameterization: An update. *J. Appl. Meteor.*, **43**, 170–181.

Kaplan, S., M. Georgescu, N. Alfasi, and I. Kloog, 2017: Impact of future urbanization on a hot summer: A case study of Israel. *Theor. Appl. Climatol.*, **128**, 325–341.

Kitao, N., M. Moriyama, S. Nakajima, T. Tanaka, and H. Takebayashi, 2009: The characteristics of urban heat island based on the comparison of temperature and wind field between present land cover and potential natural land cover. *Proceedings of the 7th International Conference on Urban Climate*, Vol. 29, Yokohama, Japan.

Kottek, M., J. Grieser, C. Beck, B. Rudolf, and F. Rubel, 2006: World map of the Köppen-Geiger climate classification updated. *Meteor. Z.*, **15**, 259–263.

Kusaka, H., 2008: Recent progress on urban climate study in Japan. *Geogr. Rev. Japan*, **81**, 361–374.

Kusaka, H., and F. Kimura, 2004: Coupling a single-layer urban canopy model with a simple atmospheric model: Impact on urban heat island simulation for an idealized case. *J. Meteor. Soc. Japan*, **82**, 67–80.

Kusaka, H., F. Kimura, H. Hirakuchi, and M. Mizutori, 2000: The effects of land-use alteration on the sea breeze and daytime heat island in the Tokyo metropolitan area. *J. Meteor. Soc. Japan*, **78**, 405–420.

Kusaka, H., H. Kondo, Y. Kikegawa, and F. Kimura, 2001: A simple single-layer urban canopy model for atmospheric models: Comparison with multi-layer and slab models. *Bound.-Layer Meteor.*, **101**, 329–358.

Kusaka, H., M. Hara, and Y. Takane, 2012: Urban climate projection by the WRF model at 3-km horizontal grid increment: Dynamical downscaling and predicting heat stress in the 2070's August for Tokyo, Osaka, and Nagoya metropolises. *J. Meteor. Soc. Japan*, **90**, 47–63.

Kusaka, H., K. Nawata, A. Suzuki-Parker, Y. Takane, and N. Furuhashi, 2014: Mechanism of precipitation increase with urbanization in Tokyo as revealed by ensemble climate simulations. *J. Appl. Meteor. Climatol.*, **53**, 824–839.

Kusaka, H., A. Suzuki-Parker, T. Aoyagi, S. A. Adachi, and Y. Yamagata, 2016: Assessment of RCM and urban scenarios uncertainties in the climate projections for August in the 2050s in Tokyo. *Climatic Change*, **137**, 427–438.

Lee, H. S., A. R. Trihamdani, T. Kubota, S. Iizuka, and T. T. T. Phuong, 2017: Impacts of land use changes from the Hanoi Master Plan 2030 on urban heat islands: Part 2. Influence of global warming. *Sustainable Cities. Soc.*, **31**, 95−108.

Li, M., T. Wang, M. Xie, B. Zhuang, S. Li, Y. Han, and N. Cheng, 2017: Modeling of urban heat island and its impacts on thermal circulations in the Beijing–Tianjin –Hebei region, China. *Theor. Appl. Climatol.*, **128**, 999–1013.

Li, X.-X., T.-Y. Koh, D. Entekhabi, M. Roth, J. Panda, and L. K. Norford, 2013: A multi-resolution ensemble study of a tropical urban environment and its interactions with the background regional atmosphere. *J. Geophys. Res.*, **118**, 9804−9818.

Lin, C.-Y., F. Chen, J. C. Huang, W.-C. Chen, Y.-A. Liou, W.-N. Chen, and S.-C. Liu, 2008: Urban heat island effect and its impact on boundary layer development and land–sea circulation over northern Taiwan. *Atmos. Environ.*, **42**, 5635–5649.

Ma, S., A. Pitman, M. Hart, J. P. Evans, N. Haghdadi, and I. MacGill, 2017: The impact of an urban canopy and anthropogenic heat fluxes on Sydney's climate. *Int. J. Climatol.*, **37**, 255–270.

Miao, S., F. Chen, M. A. LeMone, M. Tewari, Q. Li, and Y. Wang, 2009: An observational and modeling study of characteristics of urban heat island and boundary layer structures in Beijing. *J. Appl. Meteor. Climatol.*, **48**, 484–501.

Miyawaki, A., 1984: A vegetation-ecological view of the Japanese Archipelago. *Bull. Inst. Environ. Sci. Technol.*, **11**, 85–101.

Miyawaki, A., 1987: *Vegetation of Japan. Vol. 8, Tohoku*, Shibundo, Tokyo, 605 pp (in Japanese with English and German summaries).

Miyawaki, A., and S. Okuda, 1975: *Potential natural vegetation map of Japan*.

Mlawer, E. J., S. J. Taubman, P. D. Brown, M. J. Iacono, and S. A. Clough, 1997: Radiative transfer for inhomogeneous atmospheres: RRTM, a validated correlated-k model for the longwave. *J. Geophys. Res.*, **102**, 16663–16682.

Mori, K., and T. Sato, 2015: Evaluating the role of snow cover in urban canopy layer on the urban heat island in Sapporo, Japan with a regional climate model. *J. Meteor. Soc. Japan*, **93**, 581–592.

Oke, T. R., 1973: City size and the urban heat island. *Atmos. Environ.*, **7**, 769–779.

Oke, T. R., 1982: The energetic basis of the urban heat island. *Quart. J. Roy. Meteor. Soc.*, **108**, 1–24.

Peel, M. C., B. L. Finlayson, and T. A. McMahon, 2007: Updated world map of the Köppen-Geiger climate classification. *Hydrol. Earth Syst. Sci.*, **11**, 1633–1644.

Sailor, D. J., and L. Lu, 2004: A top–down methodology for developing diurnal and seasonal anthropogenic heating profiles for urban areas. *Atmos. Environ.*, **38**, 2737–2748.

Sailor, D. J., M. Georgescu, J. M. Milne, and M. A. Hart, 2015: Development of a national anthropogenic heating database with an extrapolation for international cities. *Atmos. Environ.*, **118**, 7–18.

Salamanca, F., A. Martilli, and C. Yagüe, 2012: A numerical

study of the Urban Heat Island over Madrid during the DESIREX (2008) campaign with WRF and an evaluation of simple mitigation strategies. *Int. J. Climatol.*, **32**, 2372–2386.

Salathé, E. P., L. R. Leung, Y. Qian, and Y. Zhang, 2010: Regional climate model projections for the State of Washington. *Climatic Change*, **102**, 51–75.

Shem, W., and M. Shepherd, 2009: On the impact of urbanization on summertime thunderstorms in Atlanta: Two numerical model case studies. *Atmos. Res.*, **92**, 172–189.

Shepherd, J. M., M. Carter, M. Manyin, D. Messen, and S. Burian, 2010: The impact of urbanization on current and future coastal precipitation: A case study for Houston. *Environ. Plann. B, Planning and Design*, **37**, 284–304.

Skamarock, W. C., J. B. Klemp, J. Dudhia, D. O. Gill, D. M. Barker, M. G. Duda, X. Y. Huang, W. Wang, and J. G. Powers, 2008: *A description of the advanced research WRF Version 3*. NCAR Technical Note, NCAR/TN–475+STR, 113 pp.

Sugimoto, S., T. Sato, and T. Sasaki, 2015a: Seasonal and diurnal variability in historical warming due to the urbanization of Hokkaido, Japan. *J. Geophys. Res.*, **120**, 5437–5445.

Sugimoto, S., T. Sato, and T. Sasaki, 2015b: Impact of land-use change on winter precipitation in Hokkaido, Japan. *SOLA*, **11**, 95–99.

Urban Planning Bureau, 2015: *Sendai city planning*. 18 pp.

Vitanova, L. L., and H. Kusaka, 2018: Study on the urban heat island in Sofia City: Numerical simulations with potential natural vegetation and present land use data. *Sustainable Cities Soc.*, **40**, 110–125.

Yang, B., Y. Zhang, and Y. Qian, 2012: Simulation of urban climate with high-resolution WRF model: A case study in Nanjing, China. *Asia-Pacific J. Atmos. Sci.*, **48**, 227–241.

Zhang, D.-L., Y.-X. Shou, and R. R. Dickerson, 2009: Upstream urbanization exacerbates urban heat island effects. *Geophys. Res. Lett.*, **36**, L24401, doi:10.1029/2009GL041082.

Zhang, N., Z. Gao, X. Wang, and Y. Chen, 2010: Modeling the impact of urbanization on the local and regional climate in Yangtze River Delta, China. *Theor. Appl. Climatol.*, **102**, 331–342.

Zhou, Y., and J. M. Shepherd, 2010: Atlanta's urban heat island under extreme heat conditions and potential mitigation strategies. *Nat. Hazards*, **52**, 639–668.